www.sciencetranslationalmedicine.org/cgi/content/full/5/200/200ra117/DC1

Supplementary Materials for

Blocking Macrophage Leukotriene B_4 Prevents Endothelial Injury and Reverses Pulmonary Hypertension

Wen Tian, Xinguo Jiang, Rasa Tamosiuniene, Yon K. Sung, Jin Qian, Gundeep Dhillon, Lajos Gera, Laszlo Farkas, Marlene Rabinovitch, Roham T. Zamanian, Mohammed Inayathullah, Marina Fridlib, Jayakumar Rajadas, Marc Peters-Golden, Norbert F. Voelkel, Mark R. Nicolls*

*Corresponding author. E-mail: mnicolls@stanford.edu

Published 28 August 2013, *Sci. Transl. Med.* **5**, 200ra117 (2013)
DOI: 10.1126/scitranslmed.3006674

The PDF file includes:

Supplementary Materials

Materials and Methods

HPLC-MS/MS assay

Stock solutions of LTB_4, LTC_4 and S1P (Cayman Chemical) were prepared at a concentration of 0.1 mg/ml for LTB_4 and LTC_4 and at 1 mg/ml for S1P. Composite calibration spiking solutions were prepared by diluting the combined stock solutions to final concentrations of 1334, 667, 333, 167, 66.7, 33.3, 16.67, 6.67, 3.33, and 1.67 ng/mL of LTB_4, LTC_4 and S1P. Composite standard solutions were spiked into BALF or cell media (DMEM) and processed with each batch of unknown samples. Chromatograms for standards were used to establish the characteristic retention time of each compound and to verify that the MS signal was linear for all analytes over the range of 1.67 – 1334 ng/ml in both matrices. The peak area of each analyte was calculated and plotted against the concentration of the calibration standards. Calibration curves were calculated by the least squares linear regression method using Analyst1.5.1 software. Aliquots (30 µl) were taken from each sample. LTB_4, LTC_4 and S1P in BALF or stimulated cell media were extracted by the addition of methanol (150 µl). The samples were then centrifuged, and the supernatant was transferred to HPLC vials. Ten µls of sample extracts were injected for LC–MS/MS analysis. HPLC was performed on a Shimadzu Prominence LC system at a flow rate of 300 µl/min. Chromatographic separation was performed on an Ascentis ES-Cyno 50 x 2 mm, 5 µm column (Supelco). A 3.5-min isocratic elution was performed using 50% 5 mM ammonium acetate/0.1% formic acid in water (mobile phase A) and 0.1% formic acid in acetonitrile (mobile phase B). The HPLC was directly coupled to an AB SCIEX 4000

QTRAP triple quadrupole mass spectrometer with electrospray ionization. The mass spectrometer was operated in the multiple reaction monitoring mode, using the transitions 335.16 to 194.80 m/z for LTB_4, 624.40 to 272.10 m/z for LTC_4, and 378.22 to 78.90 m/z for S1P. The elution times for LTB_4, LTC_4 and S1P were 1.6, 1.0 and 1.4 minutes, respectively. Automatic peak detection, integration and data processing were performed by the AB SCIEX Analyst 1.5.1 software package. Concentrations of LTB_4, LTC_4 and S1P were calculated by plotting the peak area of each analyte against the calibration curve prepared in corresponding matrix.

RT-PCR primers

BLT1:

forward: GCCTTCTGGCTGCCTTATCA

reverse: AGTCATGAAGCTGTCGGTGG

CysLT1:

forward: GCCTCACCACCTATGCCTTA

reverse: TCCTTCGACTTGGCAGGTTTT

LTA_4H:

forward primer: GGGACAGTACGACCTGTTGG

reverse primer: ATCGGGGTCTACGTCCTTCA

DAF-2DA(Diaminofluorescein–2 Diacetate) Staining for in vivo NO Release

DAF-2DA was purchased from Enzo Life Science. Frozen tissue sections were incubated with 1x working solution of DAF-2DA (diluting stock solution 1:250 with PBS) for 2 hrs. Sections were washed three times to remove excess dye and imaged.

DHE(Dihydroethedium) Staining for ROS Production

DHE was purchased from Invitrogen (D-23197). Tissue sections were first immuno-stained with specific cellular markers followed with incubation with 50uM DHE for 1hr at room temperature in a dark chamber. Sections were washed three times to remove excess dye. Images were captured immediately using confocal microscope.

Morphometric analysis of $iNOS^+$ macrophages, p5-LO^+ macrophages and LTA_4H^+ macrophages.

Measurements were performed using Metamorph Software on immunofluorescence confocal images. Double positive macrophages were registered (either $iNOS^+CD68^+$, p5-LO^+CD68^+ or $LTA_4H^+CD68^+$). Distance from the macrophage to the center of the nearest small arteriole (less than 100 µm in diameter) was measured and recorded. Distance was then grouped as being <50µm, 50-100µm or 100-150µm from arteriole. Finally the total number of macrophages (m1, m2, m3, etc) in each group was counted, and the percentage of double positive cells in each group was calculated (e.g., m1/(m1+m2+m3)*100).

TUNEL Staining of Lung Tissues

Click-it TUNEL Alexa Fluor 488 imaging Assay (Invitrogen) was used to detect endothelial and smooth muscle apoptosis. Briefly, tissue slides were fixed using 4% paraformaldehyde in PBS followed by a permeabilization step with 0.15% TritonX-100. TdT-mediated TUNEL reaction was carried out by covering slides in the reaction mixture for 60 mins at 37ºC, followed by Click-it reaction for 30 mins at room temperature. Slides were then proceeded to regular immunofluoresence staining protocol.

Titer TACS Colorimetric Apoptosis Assay

Titer TACS™ Colorimetric Apoptosis Detection Kit was purchased from R&D Systems (4822-96-K). Briefly, PAECs seeded on the 96 well plate were incubated with TdT labeling mixture for 60 mins at 37ºC, followed by Strep-HRP for 10 mins. Cells were then covered with TACS-Sapphire for 60 mins at room temperature in the dark. Reaction was stopped by 5% phosphoric acid. Optical density was recorded at 450nM. TACS-nuclease treatment was used as a positive control.

Macrophage Depletion using Clodronate-containing Liposomes

Clodronate is a bisphosphonate that, when injected in liposomes, is ingested by circulating macrophages. The intracellular release and accumulation of clodronate induces macrophage apoptosis. Clodronate was administered beginning 1 day before SU to prevent PH. Rats were injected intravenously with either liposomal clodronate or

liposomal vehicle biweekly for 3 weeks (15 mg/kg; Encapsula NanoScience, Nashville, TN).

MCT rat PH Model

Adult male Sprague-Dawley rats (300–350 g in body weight; Charles River Laboratories) were randomized for treatment after a s.c. injection of saline or 60 mg/kg MCT (Sigma-Aldrich) to induce pulmonary hypertension. PH was monitored by weekly ECHO. In addition to a group of untreated rats, the experimental groups include rats that received once-daily oral bestatin 0 wk, 1 wk, 2 wk or 3 wk after MCT at a dose of 1mg/kg, for a total of 5 wk, 4 wk, 3 wk or 2 wk respectively. Rats were sacrificed for hemodynamic on wk 5.

Su5416-Hypoxia (SuHx) Rat PH Model

All experimental procedures were approved by the Institutional Animal Care and Use Committee of the Virginia Commonwealth University. Adult male Sprague-Dawley rats (Harlan Laboratories, Indianapolis, IN) weighing 180 to 220 g were injected subcutaneously with SU5416 (20 mg/kg) and exposed to hypoxia (10% O2) for 4 wk. They were returned to normoxia (21% O2) for an additional 2 wk with or without bestatin treatment. PH was monitored by weekly ECHO. Rats were sacrificed for hemodynamic measurements on 6 wk.

Human Serum LTB_4 measurements.

Serum from de-identified healthy controls, iPAH patients or CTD-PAH patients was procured from the IRB-approved Stanford Pulmonary Hypertension Biobank. Serum (200 µl) was pre-treated with 20 µl of methanol/water (50/50), 6 µl of internal

standard solution (d4-LTB_4 in acetonitrile at 50 ng/ml) and 200 µl of water for extraction. The serum samples were vortexed for 30 min and loaded onto Strata X SPE columns (Phenomenex)that were conditioned with 1 ml of acetonitrile and water. The columns were washed with 1ml of 5% acetonitrile in water, and LTB_4 was then eluted with 1 ml of 5% acetonitrile in ethyl acetate. The eluent was dried under a gentle stream of nitrogen, and was dissolved in 50 µl of water-acetonitrile [50/50] for LC-MS/MS analysis.

LTB_4 was separated by reverse-phase liquid chromatography on a Thermo BDS Hypersil (50*2.1mm, 5µm particle size) column at a flow rate of 400 µl/min at room temperature. The mobile phase A was water containing 5mM ammonium acetate and 0.1 % formic acid, and the mobile phase B was 0.1 % formic acid in acetonitrile. The column was run with a 20-48% gradient of mobile phase B in 0-3min, 48% B 3-8.5min, 20% B 8.5-10min. LTB_4 was analyzed using a tandem quadrupole mass spectrometer (ABI 4000, Applied Biosystems with Shimadzu LC pumps and autosampler) via multiple reaction monitoring (MRM) in negative ion mode. The electrospray voltage was -4.5 kV, and the turbo ion spray source temperature was 550 ℃. Collisional activation of LTB_4 precursor ions used nitrogen as a collision gas. LTB_4 was measured using precursor/product (MRM) pairs. For LTB_4, the MRMs were 335/195 and 335/129; for the d4-LTB_4 the MRM was 339/197. LTB_4 was identified in samples by matching the two MRM signals and LC retention time with those of a pure standard and with the MRM of the internal standard.

Quantitative LTB_4 determination was performed by the stable isotope dilution method. Deuterated internal standard (300 pg) was added to each sample to account for extraction efficiency and mass spectrometry ion suppression. To calculate the

amount of LTB_4 in a sample, the ratio of the natural LTB_4 peak area to the deuterated LTB_4 peak area was determined for each sample. The LTB_4 ratio, proportional to concentration of LTB_4, was converted using the standard curve, and 300 pg of deuterated LTB_4 standard was mixed with the following concentrations of natural LTB_4 (nondeuterated) primary standard: 0.02, 0.05, 0.1, 0.2, 0.5, 1, 2, and 5 ng/ml in pure water. 1/x weighted linear regression was used to calculate the unknown LTB_4 concentration in a sample. All chemicals and solvents were purchased from Sigma-Aldrich or Fisher Scientific. LTB_4 was purchased from Cayman Chemicals.

Bestatin, JNJ-26993135, LY293111 and DCU biosyntheses and formulations.

Bestatin was purchased from Cayman Chemical, poly (ethylene glycol), Mw ~ 400 (PEG-400) and 2-hydroxypropyl-(□)-cyclodextrin (HPCD) were obtained from Sigma Aldrich, USA. 1-(4-(benzo[d]thiazol-2-yloxy) benzyl)piperidine-4-carboxylic acid (JNJ-26993135) and 2-[2-Propyl-3-[3-[2-ethyl-4-(4-fluorophenyl)-5-hydroxyphenoxy]propoxy]phenoxylbenzoic Acid (LY293111) were synthesized in the BioADD Facility at Stanford University. The LY293111 was synthesized using a procedure developed by Sawer et al. (*81*), purified using HPLC and then characterized by NMR and mass spectroscopies. The detailed methods of the syntheses are provided in the online supplement. Dicyclohexyl urea (DCU) was synthesized as a byproduct of a peptide coupling reaction and used after purification by recrystallization.

The oral formulation for bestatin was prepared by adding 100 µL of PEG-400 to 100 mg of bestatin, and gently mixed into a suspension. A 20% (w/v) aqueous solution of HPCD was added to bring the volume to 50 mL. The solution was vortexed and sonicated at room temperature to obtain a clear/homogeneous solution at 2mg/mL

concentration. The oral formulations for JNJ-26993135, LY293111 and DCU were prepared by the same method. The final concentration of JNJ-26993135 was 6mg/mL, LY293111 was 2mg/mL and DCU was 2mg/mL, and then appropriate dilutions were made from these stock solutions.

Detailed Methods for the Synthesis of JNJ-26993135 (LTA_4H inhibitor)

A new and efficient means of synthesizing this compound was created for the current study in collaboration with the BioADD Laboratory at Stanford. This is now the subject of a separate manuscript, currently in preparation, and this new protocol is briefly summarized below:

Synthesis of JNJ-26993135: 1-(4-(benzo[d]thiazol-2-yloxy) benzyl) piperidine-4-carboxylic acid:

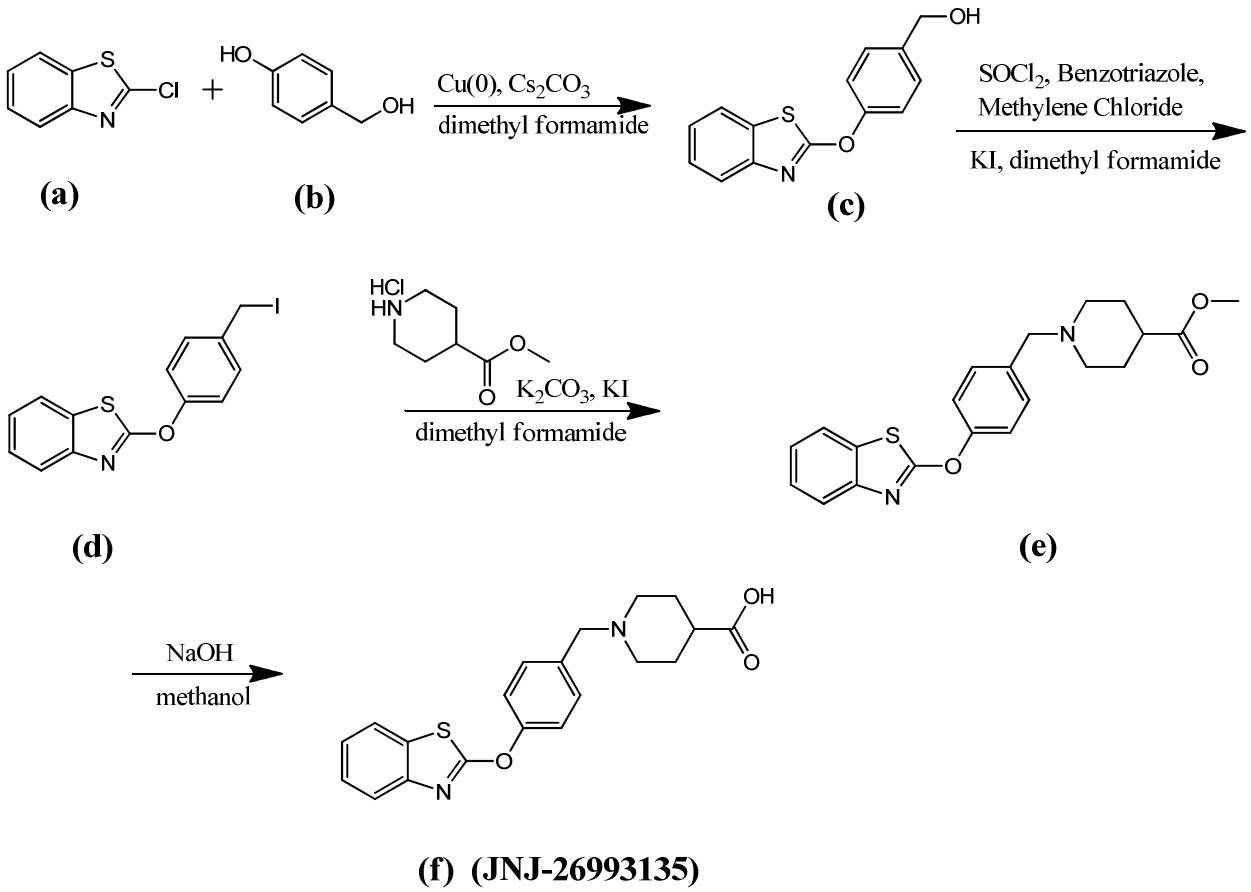

(a) **(b)** **(c)** **(d)** **(e)**

(f) (JNJ-26993135)

(1) 4-(benzo[d]thiazol-2-yloxy)phenyl)methanol **(c):** 2-chlorobenzo[d]thiazole **(a)** (2.535g, 15 mmol) and 4-Hydroxy benzyl alcohol **(b)** (2.78 g 22.4 mmol) were suspended in dimethyl formamide (DMF) (33 ml) in a 100 mL round bottomed flask over an oil bath with condenser to this copper powder (950 mg, 1.5 mmol, Aldrich 99%, 1), and cesium carbonate (14.5 g, 4.45 mmol) and heated with stirring under nitrogen atmosphere for 18 hrs. After completion of the reaction the DMF was evaporated in rotary evaporator and the residue was solubilized in ethyl acetate and washed with 1N NaOH and then water. The organic layer was dehydrated using sodium sulfate anhydrous to get 80% compound [(4-(benzo[d]thiazol-2-yloxy)phenyl)methanol]**(c)** observed as a single spot in thin layer chromatography (TLC).

(2):2-(4-(iodomethyl)phenoxy)benzo[d]thiazole **(d):** A mixture of 10 mmol (4-(benzo[d]thiazol-2-yloxy)phenyl)methanol(1), 11 mmol of thionyl chloride, and 10 mmol of benzotriazole in 20 mL of DMF was stirred for 5min. Then 10 mmol of potassium iodide in 20 mL of DMF were added to this mixture and stirred until the reaction was complete (TLC, 10 min). The product was extracted with 3X 20 mL of ether, washed with 7 mL of aq. sodium thiosulfate (5%), and 3X 30 mL of distilled water. The organic layer was dried with sodium sulfate and the solvent removed under reduced pressure. The purification of crude compound yielded 70% of iodide derivate [2-(4-(iodomethyl)phenoxy) benzo[d]thiazole] **(d)**.

*(3) [ethyl 1-(4-(benzo[d]thiazol-2-yloxy)benzyl)piperidine-4-carboxylate]***(e):** To a stirred mixture of 2-(4-(iodomethyl)phenoxy)benzo[d]thiazole, **(d)** (3 g, 15 mmol), potassium carbonate (4.14 g, 15 mmol), and potassium iodide (0.92 g, 5.6 mmol) in DMF (120 mL) was added piperidine-4-carboxylic acid ethyl ester (4.6 g, 30 mmol). The reaction mixture was heated to 90 ℃ for 16 hrs. Af ter cooling to room temperature, the mixture was diluted with water (120 mL) and stirred for 2 hrs. The supernatant liquid was decanted from the resulting residue, and was purified by preparative (~250 g of SiO2, 5 % methanol/methylene chloride, gradient) to provide 60% of the target compound [ethyl 1-(4-(benzo[d]thiazol-2-yloxy)benzyl)piperidine-4-carboxylate] **(e)**.

The above compound [ethyl 1-(4-(benzo[d]thiazol-2-yloxy)benzyl)piperidine-4-carboxylate] **(e)** was hydrolyzed by stirring with of 1N NaOH for 60 min, neutralized using IN HCl and then evaporated under vacuum to obtain the final compound [1-(4-(benzo[d]thiazol-2-yloxy)benzyl)piperidine-4-carboxylic acid] **(f)** JNJ-26993135. The final compound was then purified using HPLC.

Brief outline of synthesis of LY293111 (BLT1 antagonist)

LY293111 was synthesized in Stanford's BioADD facility using a procedure developed by Sawyer et al (*89*) with minor modifications. The LY293111 molecule was constructed from two starting materials: 4-(benzyloxy)-2-hydroxyacetophenone and 1,3-dimethoxybenzene. The procedures involved multi step syntheses of two fragments. Products at each step of the reactions were purified using chromatographic methods and were characterized by NMR spectroscopy. The two fragments were then coupled and the functional groups were deprotected to obtain the final product LY293111 which was purified using HPLC and then characterized by NMR and mass spectroscopy.

Detailed Methods of Synthesis of LY293111 (BLT1 antagonist) adapted from (89)

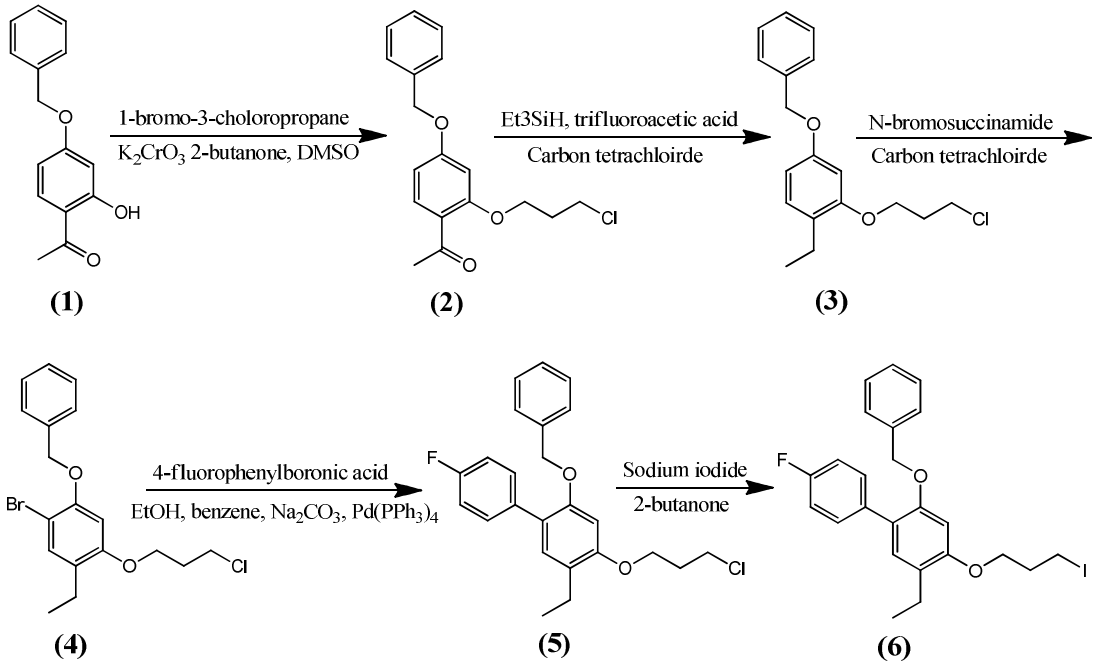

4-(Benzyloxy)-2-(3-chloropropoxy)acetophenone **(2).** A mixture of 4-(benzyloxy-2-hydroxy acetophenone **(1)** (150 mg, 0.618 mmol): 1-bromo-3-chloropropane (0.25 mL.

2.46 mmol), potassium carbonate (166 mg, 1.20 mmol), and methyl sulfoxide (1.2 mL) in 2-butanone (5 mL) was refluxed for 24 hrs. The reaction mixture was cooled and filtered. The mixture was concentrated in vacuo, diluted with ethyl acetate, and washed twice with water and twice with saturated sodium chloride solution. The organic layer was dried (magnesium sulfate), filtered, and concentrated *in vacuo*. Silica gel chromatography (ethyl acetate methylene chloride) of the resulting oil provided 162 mg of the product as a white crystalline solid.

4-(Benzyloxy)-2-(3-chloropropoxy)ethylbenzene **(3).** To a solution of compound **(2)** (120.mg. 316 µmol) in carbon tetrachloride (3.0 mL) were added trifluoroacetic acid (444 mg, 3.9 mmol) and triethyisilane (218 mg. 1.88 mmol). The mixture was stirred at room temperature for 1.5 hrs. then diluted with ethyl acetate, and washed with aqueous sodium carbonate. The organic layers were collected dried (magnesium sulfate) filtered and concentrated in vacuo. Silica gel chromatography provided 106 mg as clear oil.

4-(Benzyloxy)-5-bromo-2-(3-chloropropoxy)ethylbenzene **(4)**. Bromination of compound **(3).** To a stirred solution of compound (3) (106 mg, 289 µmol) in carbon tetrachloride (10 mL) was added N-bromosuccinimide (60 mg. 330 µmol). Stirring was continued for 6 hrs at room temperature. The mixture was then diluted with methylene chloride and washed once with water. The organic layer was dried (magnesium sulfate) filtered, and concentrated in vacuo. The residue was recrystallized from hexane/ethyl acetate to provide 102mg of compound as a crystalline solid.

4-(Benzyloxy-2-(3-chloropropoxy)-5-(4-fluorophenyl)-ethylbenzene **(5).** In a round-bottom flask was placed a solution of the compound **(4)** (260 µmol) in 5mL. To this solution were added Pd $(PPh_3)_4$ (26 µmol) and 2.0 M aqueous sodium carbonate

solution (2 mL). In a separate flask, (4-fluorophenyl) boronic acid (389 µmol) was dissolved in ethanol (2mL). To the aryl boronic acid solution was added the aryl bromide solution, and the resulting mixture was heated to reflux with stirring for 16 hrs. The mixture was diluted with ethyl acetate and washed once with saturated aqueous ammonium chloride solution. The organic layers were dried (magnesium sulfate), filtered and concentrated in vacuo. The residue was purified by silica gel chromatography to provide 87 mg of product as a crystalline solid.

4-(Benzyloxy)-5-(4-fluorophenyl)-2-(3-iodopropoxy)ethylbenzene **(6).** A mixture of compound **(5)** (80 mg, 200 µmmol) and sodium iodide (300mg, 2 mmol) in 2-butanone (8 mL) was refluxed for 6 h. The reaction mixture was cooled to room temperature, diluted with an equal volume of ether, and washed once with water. The organic layer was dried (sodium sulfate), filtered, and concentrated in vacuo to provide 84 mg of product as colorless oil.

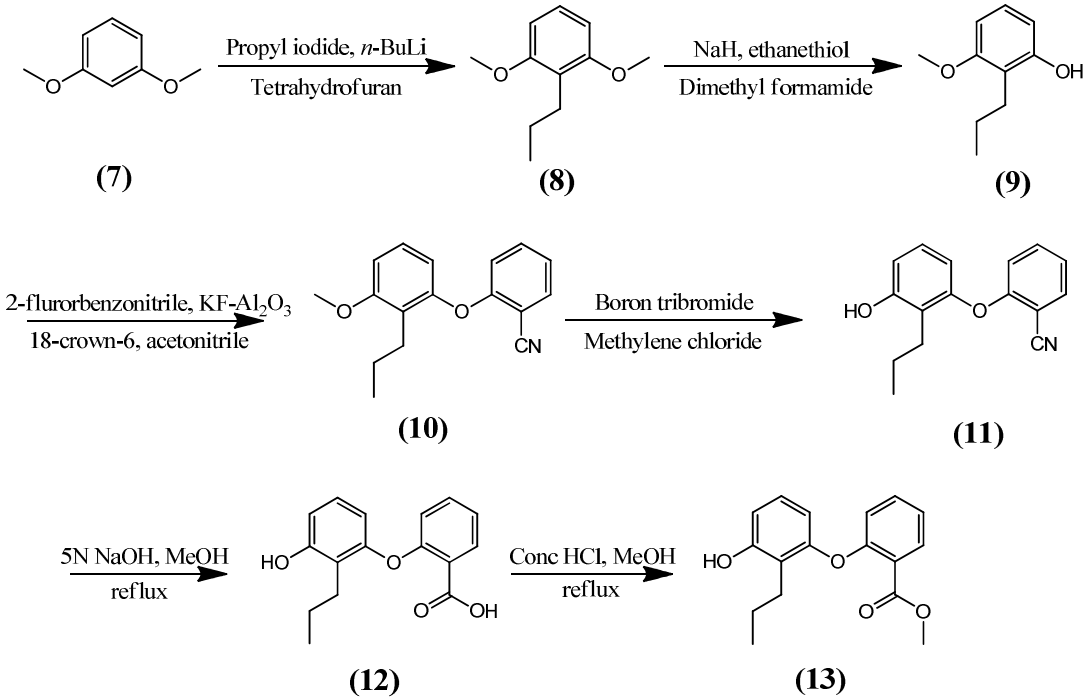

1,3-Dimethoxy-2-propylbenzene **(8)**. To a solution of 1,3-dimethoxybenzene **(7)**, (160 mg, 1.10 mmol) in tetrahydrofuran (16 mL) cooled to -70℃ was added *n*-butyllithium in hexane (1.28 mmol) at a rate which maintained the temperature of the reaction mixture at less than -45℃. When addition was complete, the mixture was allowed to warm to room temperature and stirred for 2 h. The mixture was cooled (to -10℃) and 1-iodopropane (197 mg. 1.16 mmol) added dropwise. The mixture was allowed to warm to room temperature and stirred for 18 h. The mixture was then refluxed for 5 h, cooled to -10℃, and carefully treated with methanol and ice water. The resulting mixture was extracted twice with 100 mL portions of ether. The combined organic layers were dried (magnesium sulfate), filtered, and concentrated in vacuo. The crude product was passed through a short pad of silica eluting with 80% hexane/20% ethyl acetate. Concentration of the combined washings in vacuo provided 194 mg of pure product.

3-Methoxy-2-propylphenol **(9)**. To a suspension sodium hydride (90.75 mg, 3.75 mmol, in dry DMF (10 mL) at room temperature was carefully added a solution of ethanethiol (200 mg, 3.0 mmol) dissolved in a minimum of DMF. After stirring for 5 min, compound (8) (190 mg, 1 mmol) was added and the resulting mixture stirred for 48 h. The reaction mixture was cooled to 0℃ and treated with 10% aqueous hydrochloric acid (5 mL). The mixture was diluted with ethyl acetate and washed three times with water. The combined aqueous layers were extracted once with ether. The combined organic layers were dried (sodium sulfate), filtered, and concentrated in vacuo to provide 165 mg of product as oil.

2-(3-Methoxy-2-propylphenoxy)benzonitrile **(10).** A mixture of compound **(9)** (165 mg. 993 µmol), 2-fluorobenzonitrile (120 mg, 993 µmol), 37% potassium fluoride-alumina (165 mg), and 18-crown-6 (26.4 mg, 100 µmol) in acetonitrile (5 mL) was refluxed for 48 h. The mixture was cooled to room temperature, filtered, and diluted with ethyl acetate. The organic layer was washed once with saturated potassium chloride solution, dried (sodium sulfate), filtered, and concentrated in vacuo to provide 260 mg of pure product as oil.

3-(2-Cyanophenoxy)-2-propylphenol **(11)**. To a solution of compound **(10)** (260 mg, 1 mmol) in methylene chloride 10 mL, at -78℃ w as added boron tribromide (0.3 mL, 3.2 mmol) dropwise via syringe. The resulting mixture was allowed to warm to -15℃, and the reaction was followed to completion v ia TLC. The mixture was filtered and concentrated in vacuo at room temperature. The residue was dissolved in ethyl acetate and washed once with water. The organic phase was dried (sodium sulfate), filtered, and concentrated in vacuo. Silica chromatography (hexane, ethyl acetate) provided 130 mg of product as white crystalline material.

2-(3-Hydroxy-2-propylphenoxy)-benzoic Acid Methyl Ester **(13).** Compound **(11)** (130 mg, 0.51 mmol) was dissolved in methanol (5 mL) and treated with 5 N aqueous sodium hydroxide solution at reflux for 48 h. The mixture was cooled to room temperature and carefully neutralized with 5N aqueous hydrochloric acid. Addition of a slight excess of acid resulted in precipitation of a crystalline material **(12)** which was collected via vacuum filtration. This material was dissolved in methanol (10 mL1 and treated with concentrated sulfuric acid (0.20 mL) at reflux for 18 h. The mixture was cooled to room temperature and diluted with ether and water. The organic phase was separated and

washed once with saturated sodium bicarbonate solution, dried (sodium sulfate), filtered, and concentrated in vacuo to provide 120 mg of product as a white solid.

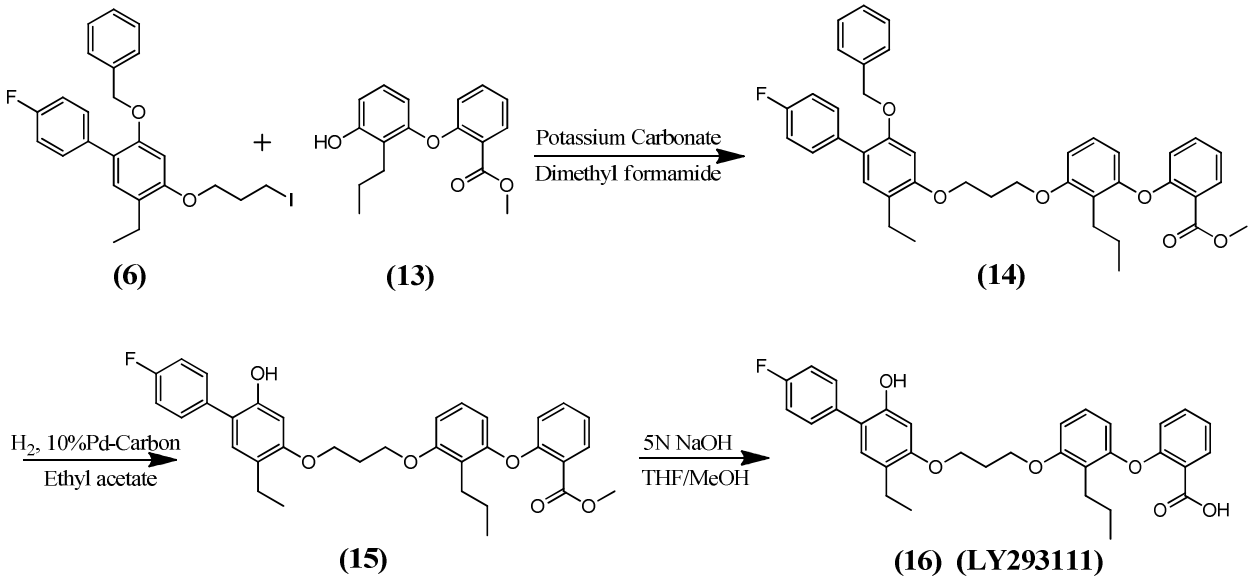

2-[2-Propyl-3-[3-[5-(benzyloxy)-2-ethyl-4-(4-fluorophenyl) phenoxy] propoxy] phenoxy] benzoic Acid Methyl Ester **(14).** A mixture of compound **(6)** (84 mg, 180µmol), compound **(13)** (51.5 mg, 180 µmol), and potassium carbonate (58.8 mg, 427 µmol) in dimethylformamide (5 mL) was stirred at room temperature for 24 h. The reaction mixture was diluted with water and extracted once with ethyl acetate. The organic layer was dried (sodium sulfate), filtered, and concentrated in vacuo. Purification via silica gel flash chromatography provided 47.3 mg of pure product as pale golden oil.

2-[2-Propyl-3-[3-[2-ethyl-4-(4-fluorophenyl)-5-hydroxyphenoxy] propoxy]phenoxylbenzoic Acid Sodium Salt **(16)**. Compound **(14)** (50.9 mmol) was debenzylated **(15)** and hydrolyzed to provide final product **(16)** LY293111.

Debenzylation: To a solution of compound **(14)** in ethyl acetate was added 10% Pd-carbon (10% wt/wt). The atmosphere of the reaction was exchanged for hydrogen

gas (1 atm) and the reaction mixture stirred at room temperature for 24 h. The dispersion was filtered over Celite and washed with ethyl acetate 5 times. The resulting solution was concentrated in vacuo and purified by silica gel chromatography to provide the compound **(15)**.

Hydrolysis: A solution of compound **(15)** in tetrahydrofuran (2.5 mL) and methanol (2.5 mL) was treated with 5N sodium hydroxide solution (1 mL) with stirring at room temperature for 1 h. The reaction mixture was concentrated in vacuo, diluted with water, and acidified to pH 1 with 5N hydrochloric acid. The resulting suspension was extracted with ethyl acetate. The organic layer was dried (magnesium sulfate), filtered, and concentrated in vacuo. The crude acid was dissolved in a minimum of 1 N sodium hydroxide solution and purified on preparative TLC to provide 21.2 mg of product as a white amorphous solid.

Pharmacokinetic analysis of oral bestatin in PH rats.

Bestatin was administered orally at 4 different doses (0.25mg/kg, 0.50mg/kg, 0.75mg/kg, 1.0 mg/kg) to rats that were injected with SU for 3 weeks. Blood samples were taken at 0 min, 10 min, 20 min, 30 min, 1h, 2h, 6h, 12h, 18h, 24h after oral administration. LC-MS/MS analysis was used to quantitate the plasma levels of the Bestatin, relative to standard curves generated in the same matrix. Pharmacokinetic parameters were determined from the data using PKSolver 2.0, (Microsoft Excel add-on). n=3 per group.

Bestatin- polyvinyl alcohol (PVA) dry powder formulation for inhalation

Dry powder bestatin-PVA microparticles were obtained by precipitating micro droplets of a precursor solution into a container of continuously stirred acetone using a spray type aerosol nozzle. To obtain the precursor solution, 1.5 g of polyvinyl alcohol (75 wt %, Sigma-Aldrich, Mr average ~ 30000), 200 mg of polyvinyl pyrrolidone (10 wt %, Sigma-Aldrich, Mr average ~ 10000), 100 mg of poloxamer 188 (5 wt %, Sigma-Aldrich, Mr average ~ 8400), 100 mg of L-leucine (5 wt %, Sigma-Aldrich), and 100 mg bestatin (5 wt %, Sigma-Aldrich) were dissolved in a mixture of 12.5 ml DMSO (Sigma-Aldrich) and 8.3 ml Millipore water at room temperature and stirred for 2 hrs. This was followed by 4 hrs of cold sonication (Branson 2510, 100W). The precursor solution pH was adjusted to 7, using 1N NaOH or 1N HCl (Sigma-Aldrich). The solution was sprayed using compressed air (at 25°C, 15 psig, 25 L/min) into a 1.2 L acetone bath in a glass container stirred with a magnetic stirrer at 230 rpm. The microparticles were filtered and dried under a vacuum at room temperature. The dry powder was further ground with a mortar and pestle and filtered through a 63 micron copper sieve.

Scanning electron microscope imaging of bestatin microparticles

The bestatin microparticles were characterized with a scanning electron microscope. Microparticles were placed on a silicon wafer and imaged after sputter-coating them with 100A° gold-palladium using a Denton Desk II TSC Sputter Coater (Denton Vacuum). The images were obtained using a Hitachi S-3400N VP-scanning electron microscope (Hitachi Ltd.) operated at 10–15 kV at a working distance of 8–10 mm and secondary electron detection.

Breathable drug delivery system

Breathable drug delivery was achieved using a custom made device based on fluidized bed principles. The device consists of a fluidized bed and an adapter cone for the rat's nose. A predetermined dose of breathable microparticles was fluidized with O_2 at 4 liters per minute (l/m) and isoflurane. The rats inhaled the particles under anesthesia for 5 minutes.

RT-PCR primers

TNF α:

forward: CGGGCAGGTCTACTTTGGAG

reverse: TCCAGTGAGTTCCGAAAGCC

CCR2:

forward: TAGGAAGCAGCCAGTCCA

reverse: TACTCATACGCGCTGAGACG

CX3CR1:

forward: GAACAACCGGACAGTGCAAC

reverse: GGTCCCTCTTCATGCCACAA

Supplemental Figures

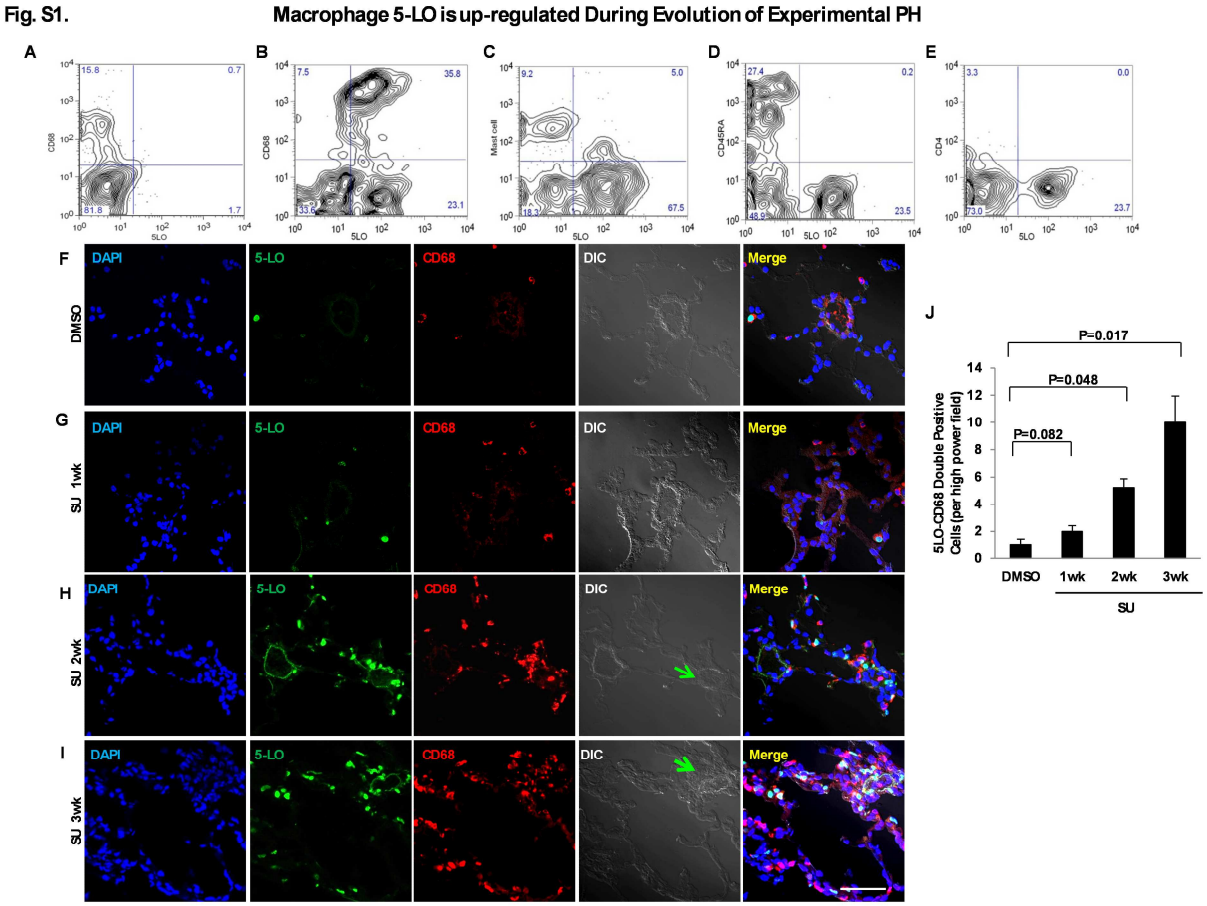

Fig. S1. Increased macrophage 5-LO during the evolution of experimental PH. Representative flow cytometry plots demonstrate double staining of CD68 (for macrophages) and 5-LO on peripheral blood mononuclear cells from (**A**) DMSO animals or (**B**) PH animals 3 wk after SU administration. Double staining of (**C**) anti mast cell and 5-LO, (**D**) CD45RA (for B cells) and 5-LO, (**E**) CD4 (for T cells) and 5-LO in cells from SU athymic PH rats (N=3 experiments per group). (**F** to **I**) Representative images demonstrate 5-LO (green) staining on CD68 (red) positive macrophages in the lung tissues, in (**F**) DMSO control group, (**G**) 1wk after SU, (**H**) 2 wk after SU and (**I**) 3 wk after SU administration. DAPI (blue), nuclei. Differential interference contrast (DIC) illustrates small lung vessel structural histology. Green arrows, center of the arterioles. (**J**) 5-LO staining during the evolution of PH in pulmonary macrophages from (F to I). 5-LO^{+} macrophages were counted as cells per high power field. N=6 per group; scale bar, 50µm. Kruskall-Wallis test followed by Dunn's multiple comparisons test for post hoc analyses were used. Data are expressed as means ± s.e.m.. NS, not significant.

Fig. S2.

Fig. S2. Tissue-specific 5-LO expression in experimental PH. Western blot analysis evaluating 5-LO expression in different solid organs 21 days after SU administration. Actin blot was used as a standard. Four independent Western analyses were performed.

Fig. S3.

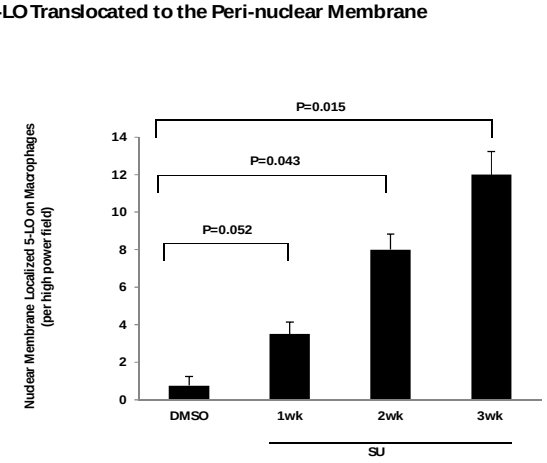

Fig. S3. **Increased nuclear membrane–translocated p5-LO over time as an indicator for 5-LO activation.** Perinuclear membrane localized p5-LO^{+} macrophages were counted per high power confocal field from Fig. S1. (F to I). N=6 per group. Kruskall-Wallis test followed by Dunn's multiple comparisons test for post hoc analyses were used. Data are expressed as means ± s.e.m. .

Fig. S4.

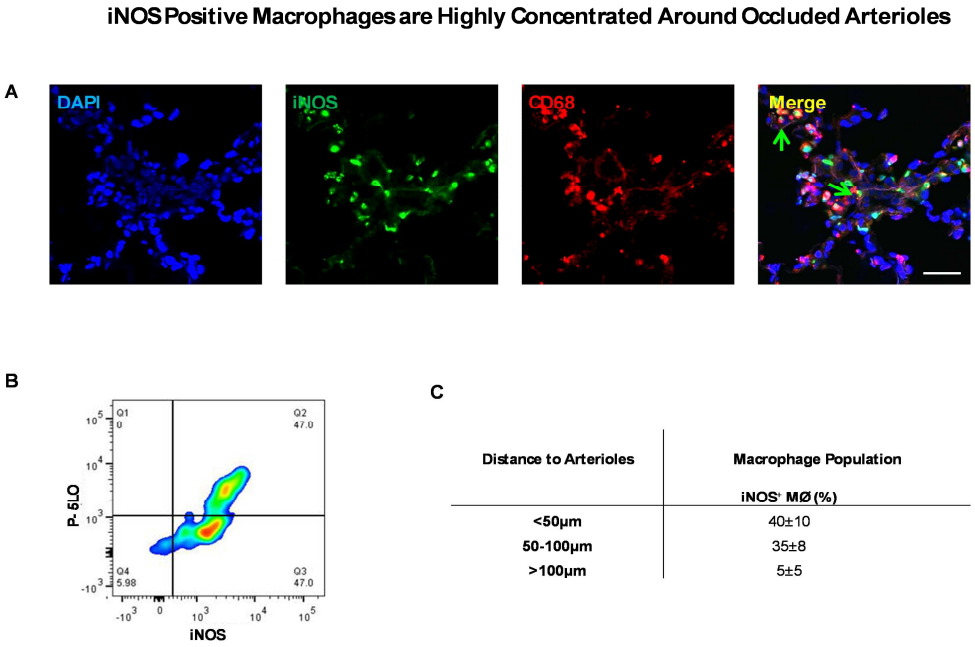

Fig. S4. High concentration of iNOS$^+$ macrophages around occluded arterioles. (**A**) Representative immunofluorescence images from SU PH lung sections stained for iNOS (green) and CD68 (red). DAPI (blue) identifies nuclei. Green arrows point to occluded arterioles. (**B**) Flow cytometry staining of interstitial lung macrophages. Cells were gated on CD68$^+$ macrophages. (p5-LO antibody was used as a surrogate marker for LTB_4 biosynthesis). (**C**) iNOS$^+$ macrophages were measured <50μm; 50-100μm or 100-150μm from centers of the small pulmonary arterioles. N=6 per group; scale bar, 50μm. Data are expressed as means ± s.e.m.

Fig. S5.

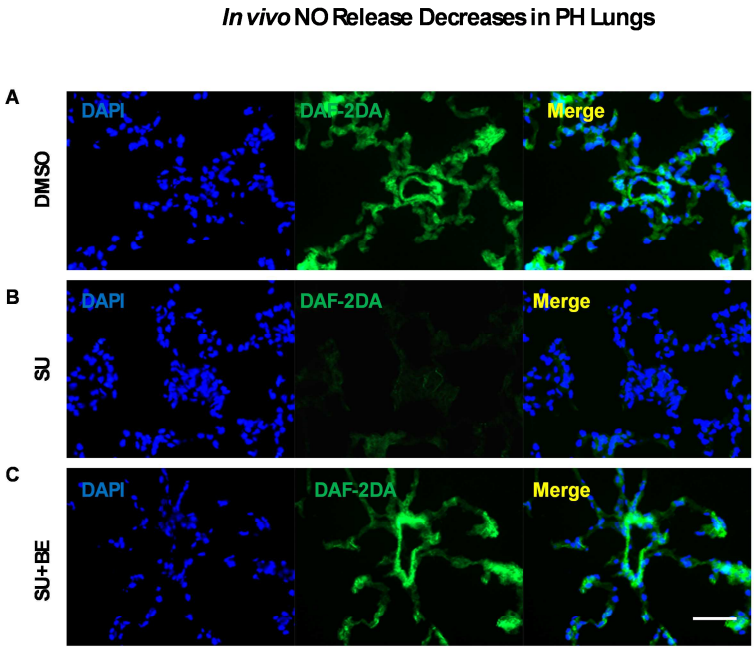

Fig. S5. In vivo NO release decreased in lungs from PH rats. DAF-2DA (green) was used to measure in vivo NO release from lung tissues obtained from (**A**) DMSO (**B**) SU and (**C**) bestatin treatment groups. NO release was detected throughout the lung tissue, and was concentrated around the pulmonary arterioles. Average tissue NO level in PH animals was significantly lower compared to DMSO and bestatin group. Representative immunofluorescence images are displayed. DAPI (blue), nuclei; N=6 per group; scale bar, 50µm.

Fig. S6.

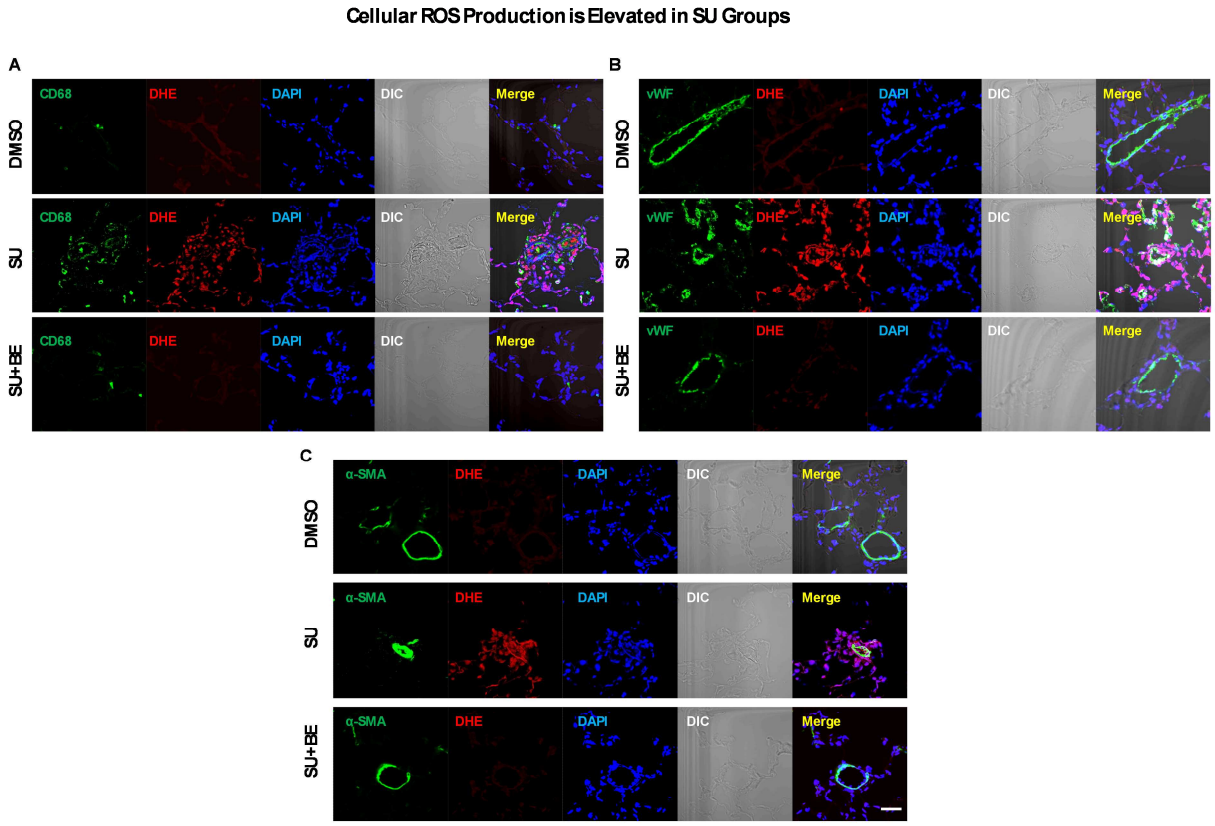

Fig. S6. Cellular ROS production is elevated in the SU group. Lung tissue ROS production was detected by DHE (Dihydroethidium) staining. Representative immunofluorescence images from DMSO, SU and bestatin lung sections co-stained for DHE (red) and different cell type markers: (**A**) CD68 (green), (**B**) vWF (green) and (**C**) *a*-SMA (green) to specify the cellular source of ROS. ROS synthesis was not restricted to particular cell types and locations. High DHE signal was observed in PH group. DAPI (blue), nuclei; N=6 per group; scale bar, 50μm.

Fig. S7.

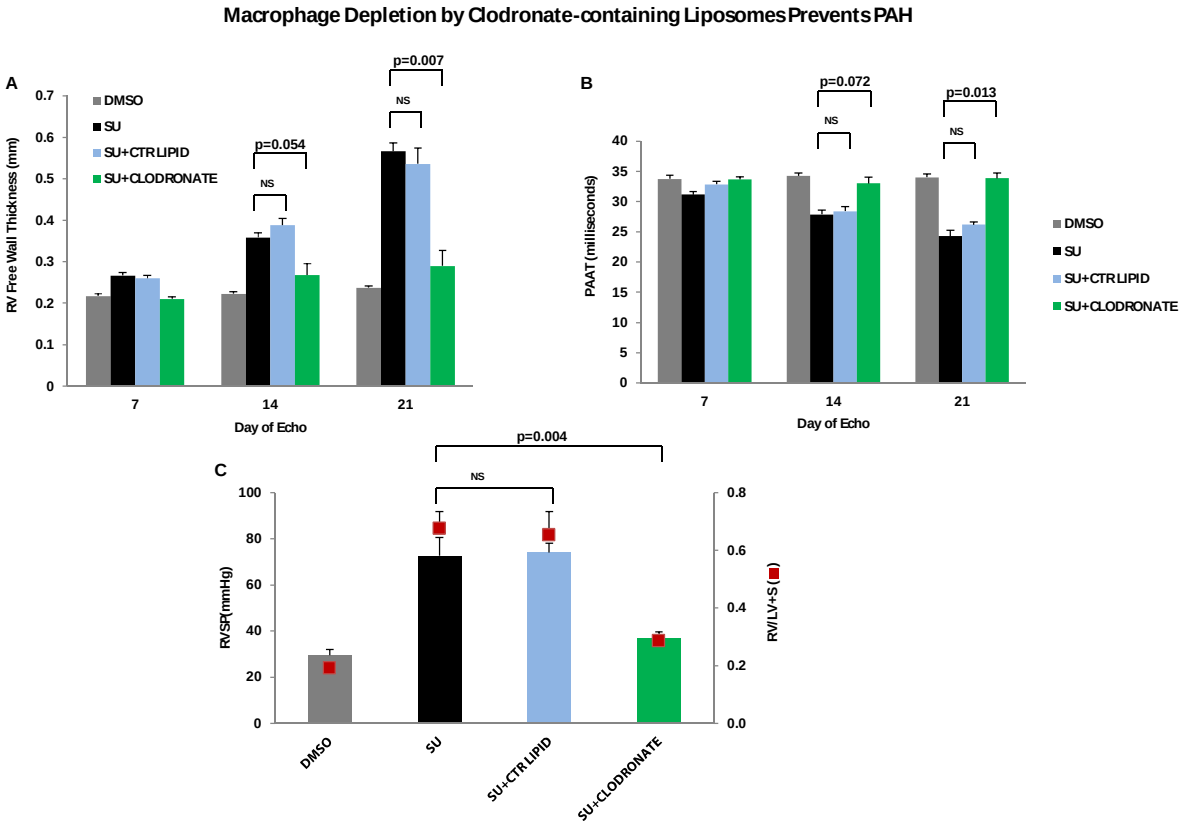

Fig. S7. Prevention of PH by macrophage depletion. Rats were injected intravenously with clodronate–containing liposomes (Cl_2MBP) bi-weekly for 3 weeks beginning 1 day before SU administration at 15mg/kg. Control liposomes were injected on the same schedule. Animals were monitored by ECHO weekly, and sacrificed for hemodynamics measurement at wk 5. (**A** and **B**) Sequential ECHO illustrating respective RV free wall thicknesses and PAAT. (**C**) Hemodynamic measurements using RVSP and RVH. N=6 per group. Two-way ANOVA with Bonferroni multiple comparisons test for post hoc analyses were used. Data are expressed as means ± s.e.m.. NS, not significant.

Fig. S8.

Interstitial Lung Macrophage (iMac)-secreted LTB_4 Induces PAEC Apoptosis

A

PAEC Flow Cytometry Groups	Mean (Annexin V⁺/PI⁻) ± SEM (%)
iMac from DMSO-treated rat lung	2.6±1.2
iMac from SU-treated rat lung	37.3± 4.7
iMac transfected with vector	1.4± 0.5
iMac transfected with WT 5-LO	4.6± 0.4
iMac transfected with S271A 5-LO	3.2± 1.1
iMac transfected with S271E 5-LO	41.1±5.1
iMac transfected with S271E 5-LO + NAC	45.0± 2.7
iMac transfected with S271A 5-LO + LTB_4	47± 4.9
LTB_4 (W/O Mac)	37.6± 3.6
LTB_4 + U75302 (W/O Mac)	4± 0.4

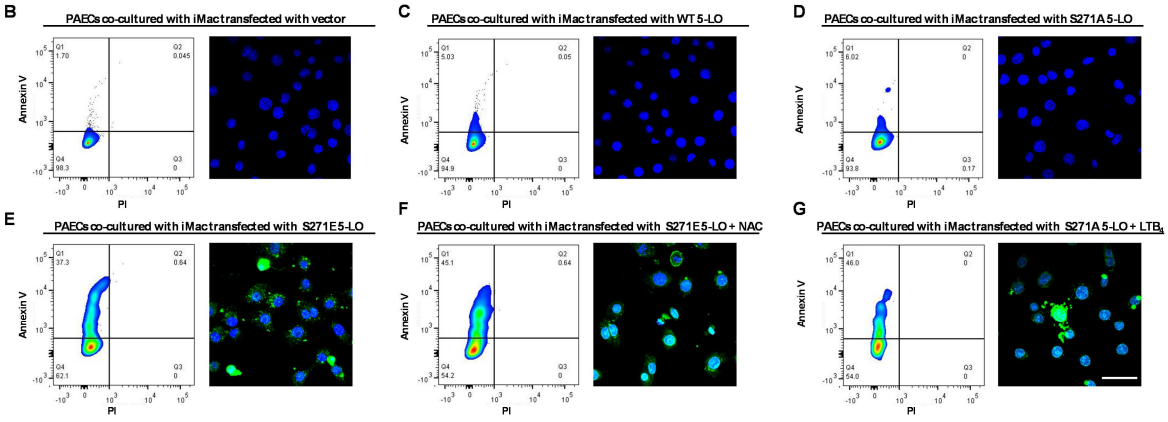

Fig. S8. Induction of PAEC apoptosis by interstitial lung macrophage (IMØ)–derived LTB_4. The transwell assay involved coculturing IMØ from several sources with PAECs. (**A**) Apoptotic population (Annexin V positive and PI negative) in (**B** to **G**) was summarized. To isolate the specific impact of LTB_4 generated by 5-LO activation on endothelial cell injury, IMØ extracted from healthy rats were transfected with S271E or S271A. Vector and WT 5-LO were used as controls. Flow cytometry for Annexin V and confocal microscopy for cleaved caspase-3 staining (green) was performed on PAECs cocultured with IMØ extracted from healthy rats and transfected with (**B**) vector, (**C**) WT 5-LO, (**D**) S271A, (**E**) S271E (**F**) S271E mutant treated with NAC (200nM) or (**G**) S271A mutant treated with LTB_4 (200nM). N=3 per group; scale bar, 50 µm. Representative flow cytometry plots and confocal images are shown. Data are expressed as means ± s.e.m..

Fig. S9.

Model and Experimental Groups of PAEC-Macrophage Co-culture System

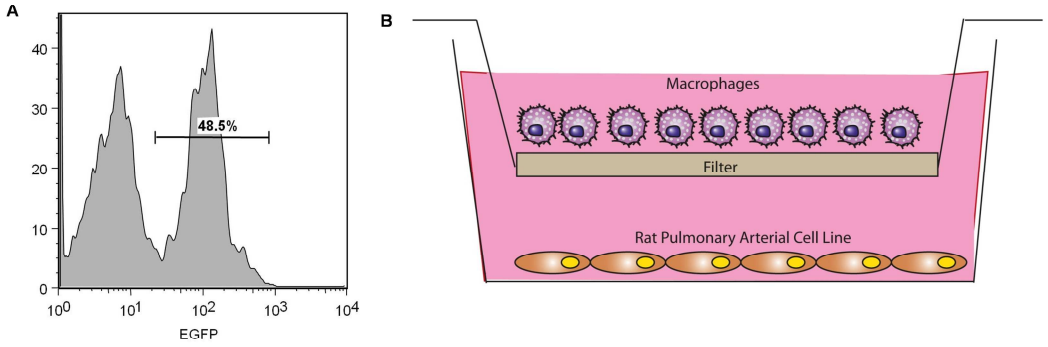

C

Macrophage	Treatment	Macrophage 5-LO	Ability to Induce Endothelial Cell Apoptosis
From digested lung or BALF of DMSO treated rats	N/A	negative control	-
From digested lung or BALF of SU treated rats	N/A	phosphorylated 5-LO	+
Transfected with vector control	N/A	negative control	-
Transfected with WT 5-LO gene	N/A	non-phosphorylated 5-LO	-
Transfected with S271A gene	N/A	dephosphorylation mimic mutant	-
Transfected with S271A gene	LTB_4	dephosphorylation mimic mutant (with exogenous LTB_4)	+
Transfected with S271E gene	N/A	phosphorylation mimic mutant	+
Transfected with S271E gene	NAC	phosphorylation mimic mutant (with anti-oxidants)	+
Transfected with S271E gene	S1P	phosphorylation mimic mutant (with exogenous S1P)	-
No macrophage	LTB_4	exogenous LTB_4	+
No macrophage	LTB_4+U75302	exogenous LTB_4 with BLT1 inhibitor	-
No macrophage	LTB_4+S1P	exogenous LTB_4 with S1P	-
No macrophage	LTC_4; LTD_4; LTE_4	exogenous LTC_4; LTD_4; LTE_4	-

Fig. S9. Experimental groups of PAEC-macrophage coculture system. (**A**) PAECs were transfected with 5-LO-eGFP constructs. Transfection efficiency was monitored with flow cytometry gated on the eGFP channel. Representative flow cytometry histogram of S271E mutant transfected macrophages is shown. (**B**) Cartoon illustrating transwell coculture system. Interstitial lung macrophages (IMØ) or alveolar macrophages (AMØ) from several sources were cocultured with PAECs for 24 hrs. Lung macrophages, from DMSO and SU-PH lungs were evaluated. To further isolate the specific impact of LTB_4 generated by 5-LO phosphorylation, macrophages were also extracted from healthy rats and transfected with S271E to produce a phosphorylation mimic mutant and with S271A to produce a dephosphorylation mimic mutant. Vector and WT 5-LO DNA-transfected macrophages were used as controls. PAECs were also treated with exogenous LTB_4, CysLTs, LTB_4 plus BLT1 inhibitor U75302, or S1P. (**C**) Results of coculture experiments are summarized below the cartoon. N=6 experiments per group.

Fig. S10.

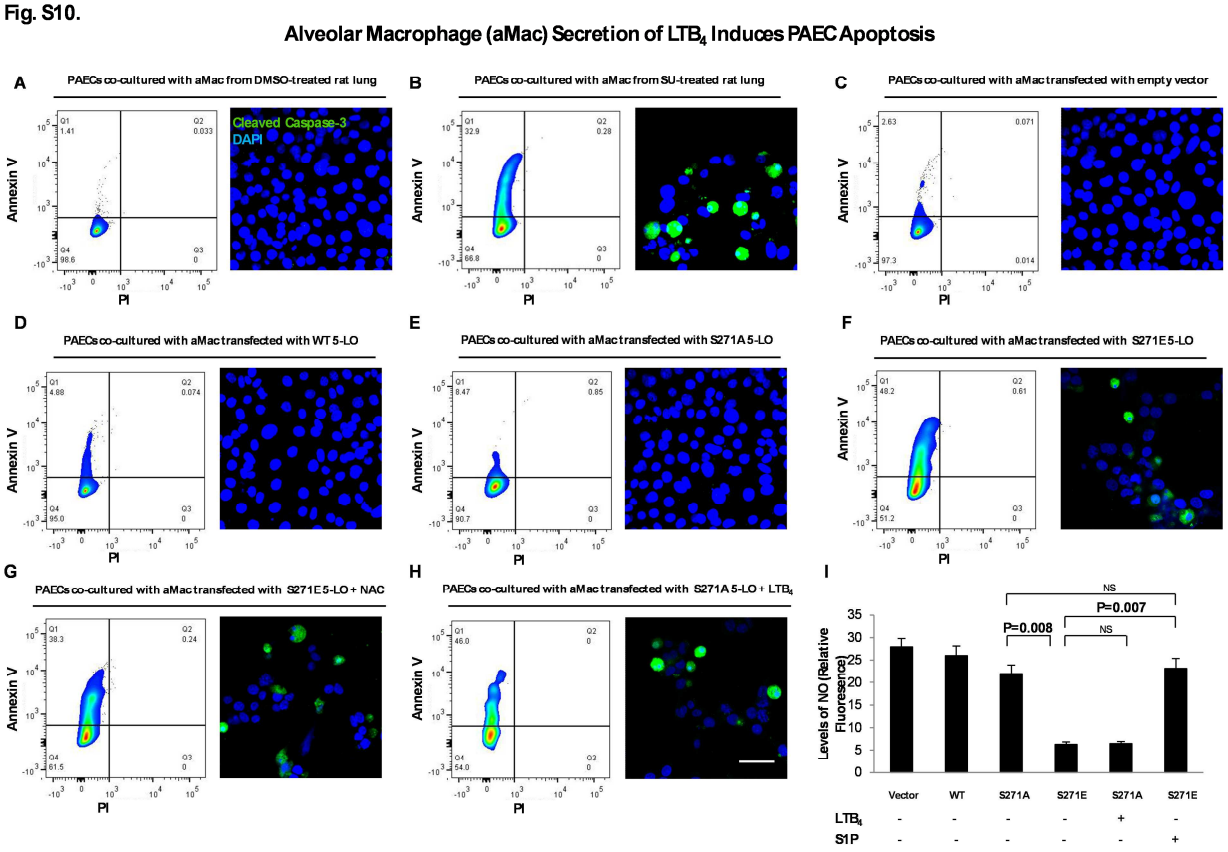

Fig. S10. Induction of PAEC apoptosis by alveolar macrophage (AMØ)–derived LTB_4. AMØ from several sources were cocultured with PAECs. After 24hr, PAEC apoptosis was analyzed by flow cytometry of Annexin V expression and by confocal microscopy for cleaved caspase-3 staining (green). (**A**) AMØ from DMSO and (**B**) SU-PH rat lungs were isolated and cocultured with PAECs. AMØ extracted from healthy rats and transfected with (**C**) vector, (**D**) WT 5-LO, (**E**) S271A (**F**) S271E, (**G**) S271E mutant treated with NAC (200nM) or (**H**) S271A mutant-treated with LTB_4 (100nM) were cocultured with PAECs. Representative flow cytometry plots and confocal images are shown. NO production from culture media in (C to H) was summarized in (**I**). N=3 experiments per group; scale bar, 50 µm. Data are expressed as means ± s.e.m.. NS, not significant.

Fig. S11.

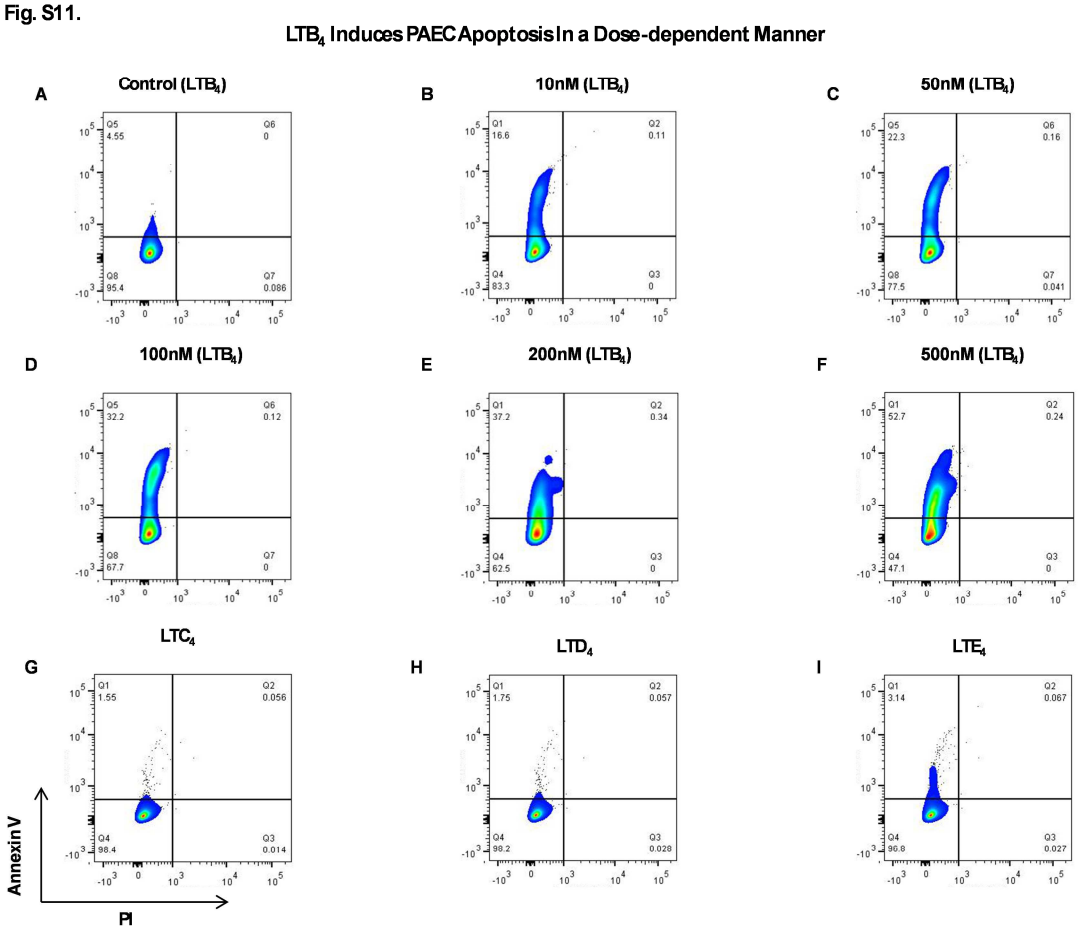

Fig. S11. LTB_4 induction of PAEC apoptosis in a dose-dependent manner. Exogenous LTB_4 was titrated at different physiologically-relevant concentrations to induce PAEC injury. LTB_4 concentrations of (**A**) 0 nM, (**B**) 10 nM, (**C**) 50 nM, (**D**) 100 nM, (**E**) 200 nM, (**F**) 500 nM were tested. Exogenously adding (**G**) 200 nM LTC_4, (**H**) 200 nM LTD_4 or (**I**) 200 nM LTE_4 had no effect on PAEC apoptosis. Annexin V and PI were used as markers for cellular apoptosis. N=3 experiments per group. Representative flow cytometry plots are shown.

Fig. S12.

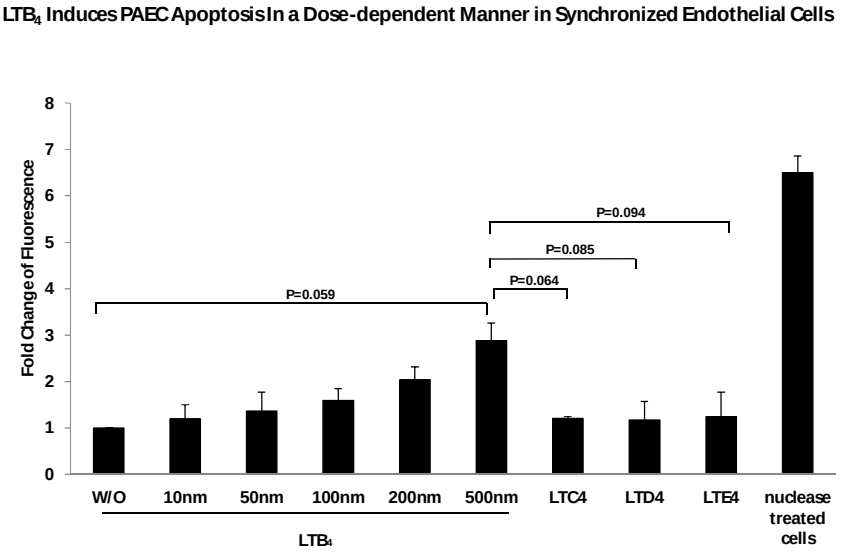

Fig. S12. LTB_4 induction of synchronized PAEC apoptosis in a dose-dependent manner. PAECs plated on a 96 well plate were synchronized by serum starvation for 24hr before exogenously adding LTB_4 to the culture. DNA fragmentation of the apoptotic cells was measured using HT TiterTACS assay system. TACS-nuclease was used as a positive control. N=3 experiments per group. Data are expressed as means ± s.e.m..

Fig. S13.

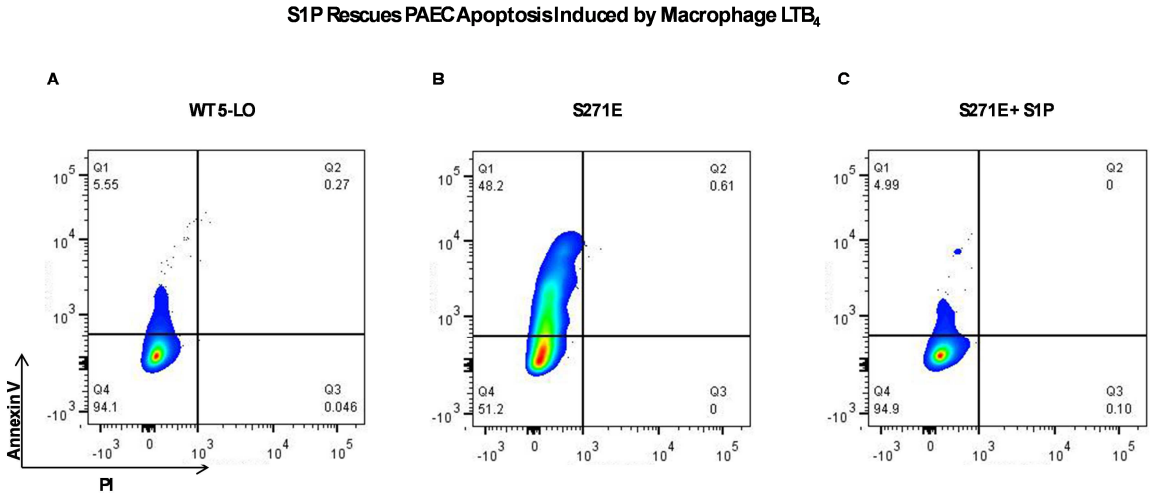

Fig. S13. S1P rescues PAEC apoptosis induced by macrophage LTB_4. Flow cytometry assessment of PAECs for apoptosis utilizing Annexin V staining. (**A**) IMØ transfected with WT 5-LO didn't induce PAEC apoptosis whereas S271E-transfected IMØ expressing high LTB4, caused significant PAEC apoptosis (**B**). (**C**) Exogenous S1P (1µM) added to coculture prevented PAEC apoptosis. N=3 experiments per group. Representative flow cytometry plots are shown.

Fig. S14. Densitometry Analysis of Western Blots

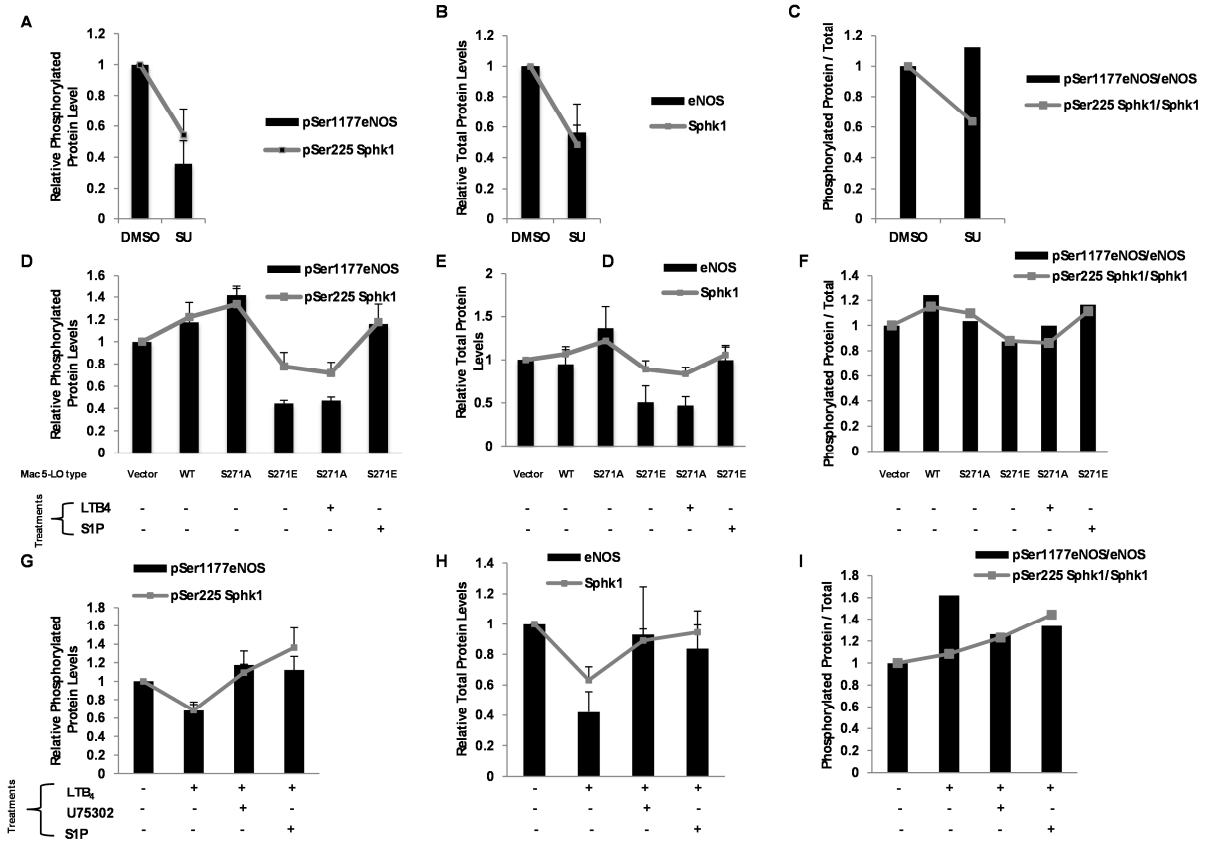

Fig. S14. Quantification of Western blots evaluating LTB_4-mediated PAEC apoptosis. Western blots in Fig. 4A, C and E were quantified using ImageJ software. Densitometry of pSer1177eNOS and pSer225Sphk1 in Fig. 4A was calculated in (**A**); densitometry of total eNOS and Sphk1 in Fig. 4A was calculated in (**B**); densitometry of pSer1177eNOS and pSer225Sphk1 in Fig. 4C was calculated in (**D**); densitometry of total eNOS and Sphk1 in Fig. 4C was calculated in (**E**); densitometry of pSer1177eNOS and pSer225Sphk1 in Fig. 4E was calculated in (**G**); densitometry of total eNOS and Sphk1 in Fig. 4E was calculated in (**H**). Intensity of phospho protein vs. total protein was calculated in **C**, **F** and **I**. N=4 per group. Data are expressed as means ± s.e.m.

Fig. S15.

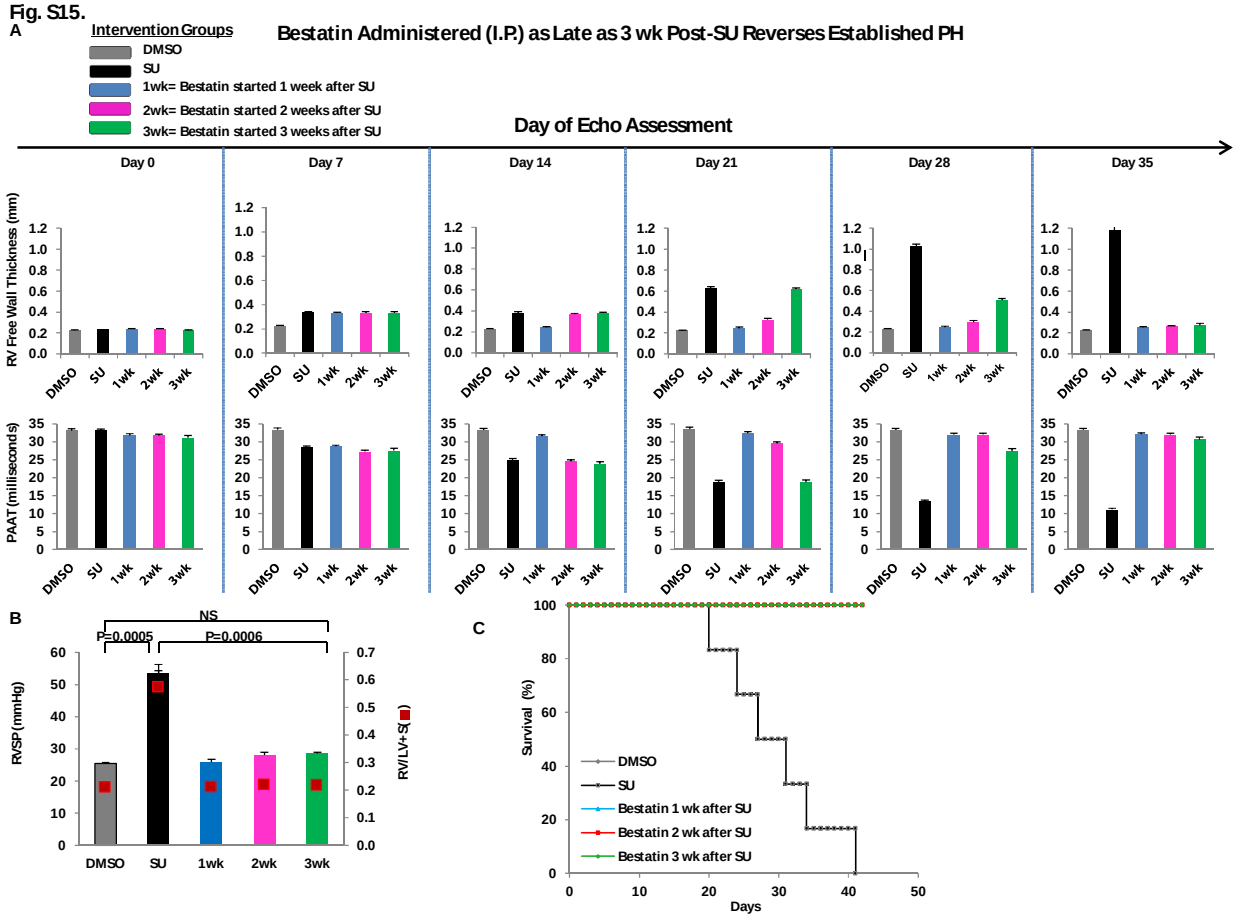

Fig. S15. The reversal of established PH by administration of bestatin 3 weeks after SU administration. Rats were injected with 8mg/kg bestatin I.P. 3 times a week starting 1wk, 2 wk or 3 wk after SU administration. Animals were monitored by ECHO weekly, and sacrificed for hemodynamics measurement at wk 5. (**A**) Sequential ECHO of DMSO, SU, bestatin (1wk after SU), bestatin (2wk after SU), and bestatin (3wk after SU) treatment groups illustrating respective RV free wall thicknesses and PAAT. (**B**) RVSP and RVH were measured in DMSO, SU, and 3 different bestatin protocols at wk 5 post-SU administration. (**C**) Kaplan-Meier survival curve. Bestatin-treated groups overlap with the DMSO (negative control) group. N=6 per group. Two-way ANOVA with Bonferroni multiple comparisons test for post hoc analyses were used. Data are expressed as means ± s.e.m.. NS, not significant.

Fig. S16.

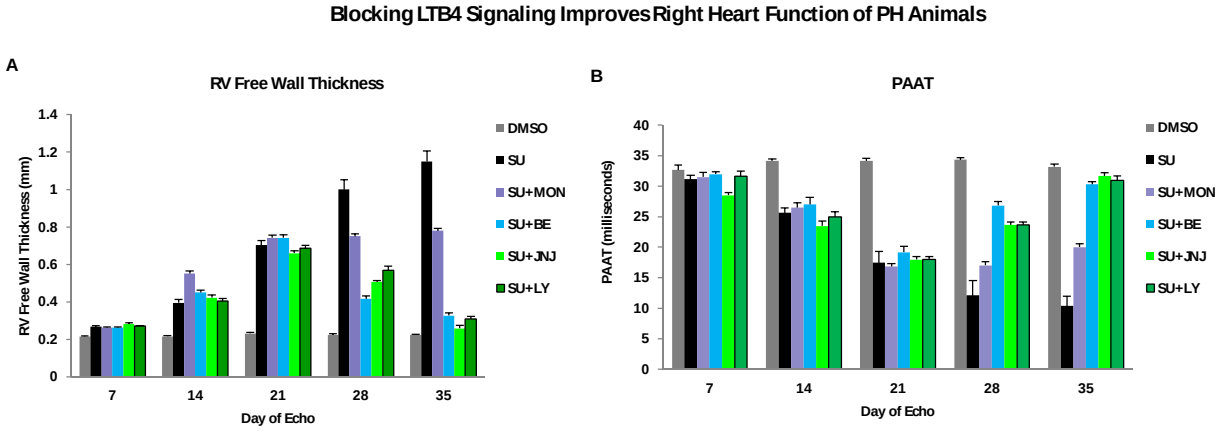

Fig. S16. The improvement of right heart function of PH animals undergoing blockade of LTB_4 signaling. Animals were monitored by ECHO weekly. (**A** and **B**) Sequential ECHO of DMSO, SU, and the treatment groups: CysLT1 receptor antagonist montelukast (MON); LTA_4H inhibitor bestatin (BE); LTA_4H inhibitor JNJ-26993135(JNJ) or BLT1 antagonist LY-293111(LY). N=6 per group. Data are expressed as means ± s.e.m..

Fig. S17.

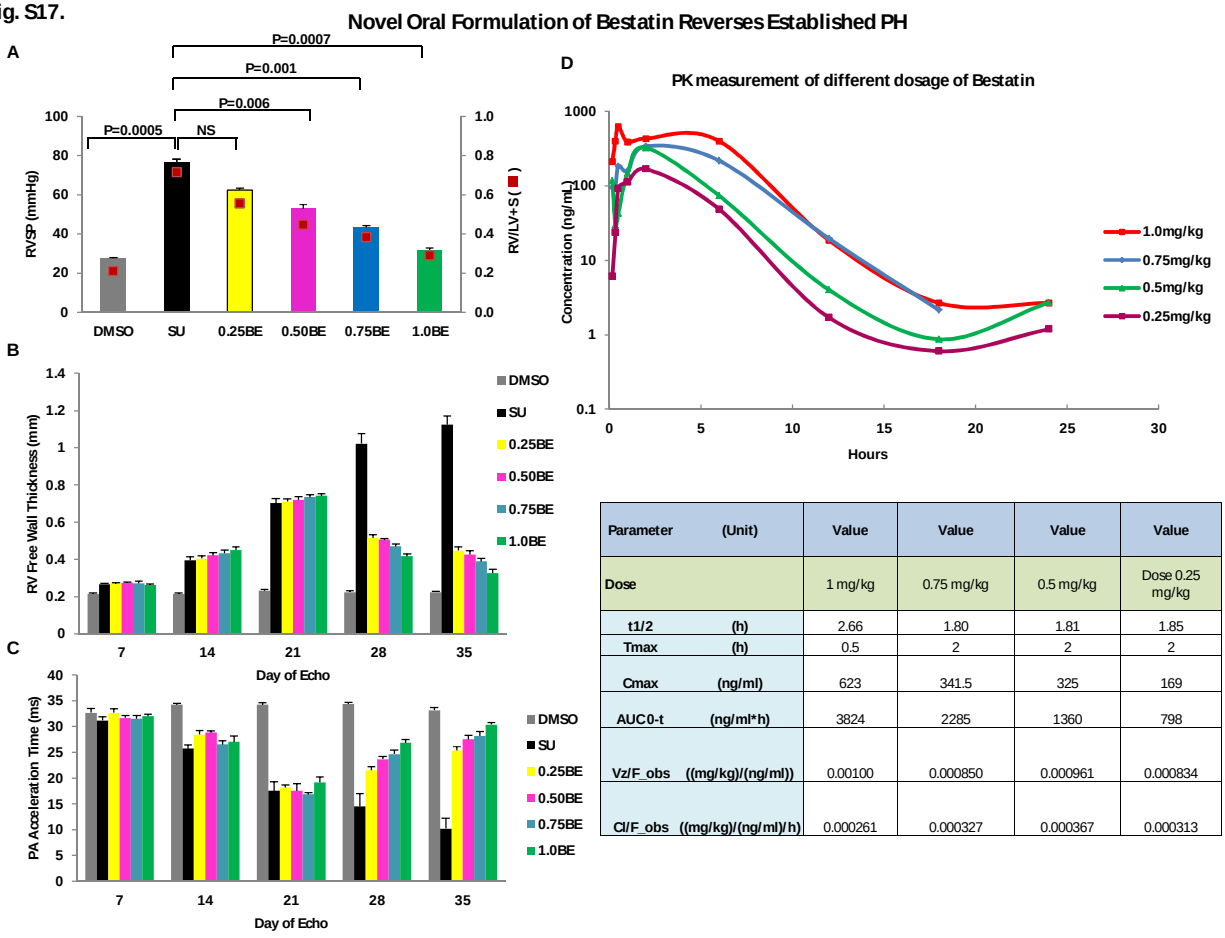

Parameter	(Unit)	Value	Value	Value	Value
Dose		1 mg/kg	0.75 mg/kg	0.5 mg/kg	Dose 0.25 mg/kg
t1/2	(h)	2.66	1.80	1.81	1.85
Tmax	(h)	0.5	2	2	2
Cmax	(ng/ml)	623	341.5	325	169
AUC0-t	(ng/ml*h)	3824	2285	1360	798
Vz/F_obs	((mg/kg)/(ng/ml))	0.00100	0.000850	0.000961	0.000834
Cl/F_obs	((mg/kg)/(ng/ml)/h)	0.000261	0.000327	0.000367	0.000313

Fig. S17. The dose-dependent reversal of established PH using novel oral formulations of bestatin. Bestatin was encapsulated with FDA proved hydroxypropoyl-β-cyclodextrin (HPCD) as a novel oral formulation to improve slow and sustain delivery. Rats were treated with 0.25, 0.50, 0.75, or 1.0 mg/kg new bestatin formulation P.O. daily 3 wk after SU administration (when PH is established). Animals were sacrificed for hemodynamics measurements (**A**) RVSP and RVH at wk 5 post-SU administration. Disease progression was monitored by ECHO weekly. (**B** and **C**) Sequential ECHO demonstrated dose-dependent efficacy of bestatin improving right heart function. (**D**) Oral availability of the new bestatin formulation was measured by pharmacokinetics. N=6 per group. Two-way ANOVA with Bonferroni multiple comparisons test for post hoc analyses were used. Data are expressed as means ± s.e.m.. NS, not significant.

Fig. S18.

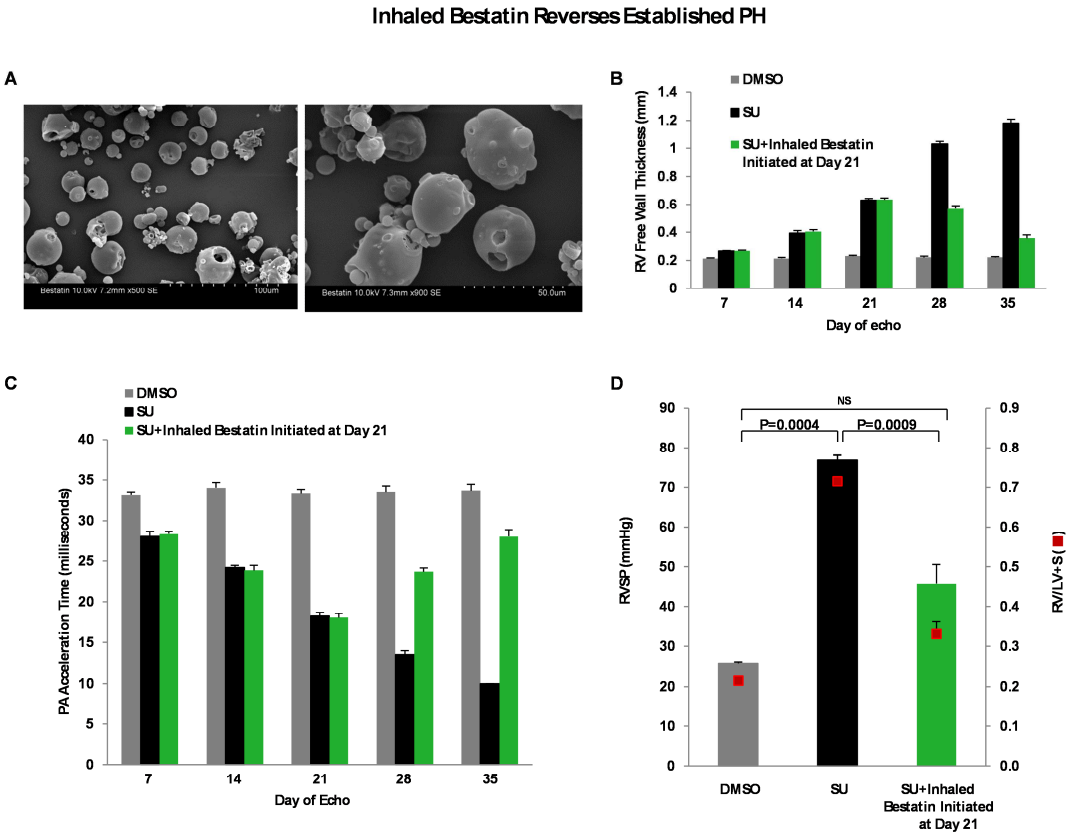

Fig. S18. The reversal of established PH using a novel formulation of inhaled bestatin. Inhalable bestatin was administered three times per week and initiated 3 wk after SU injection. (**A**) Scanning electron microscopy images of the breathable bestatin particles. Particles were coated with Au-Palladium (10 nm) before imaging. Average size of the particles is approximately 30 microns. (**B** and **C**) Sequential ECHO at different time points. (**D**) Measurements of hemodynamics were performed at wk 5. N=6 per group. Two-way ANOVA with Bonferroni multiple comparisons test for post hoc analyses were used. Data are expressed as means ± s.e.m.. NS, not significant.

Fig. S19.

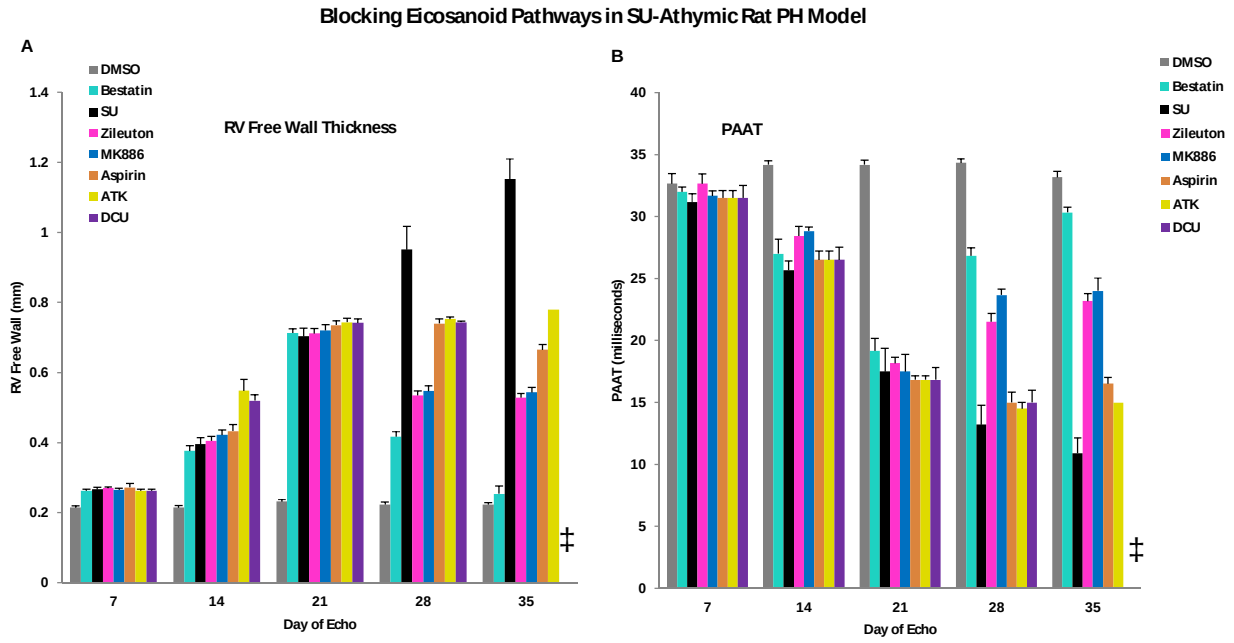

Fig. S19. Blocking multiple eicosanoid pathways in the SU/athymic rat PH model. To further examine the specific contribution of LTB_4 to PH pathogenesis, compounds that block additional eicosanoid signaling pathways were used. Rats were treated with PLA_2 inhibitor, ATK; 5-LO inhibitor, Zileuton; FLAP inhibitor, MK886; COX inhibitor, aspirin; EET inhibitor, DCU; LTA_4H inhibitor, bestatin (following the dosing regimen listed in table S2) starting 3 wk after SU administration. Animals were monitored by ECHO (**A** and **B**). N=6 per group. ‡ All animals were dead by the day of terminal right heart catheterization in wk 5. Data were expressed as means ± s.e.m..

Fig. S20.

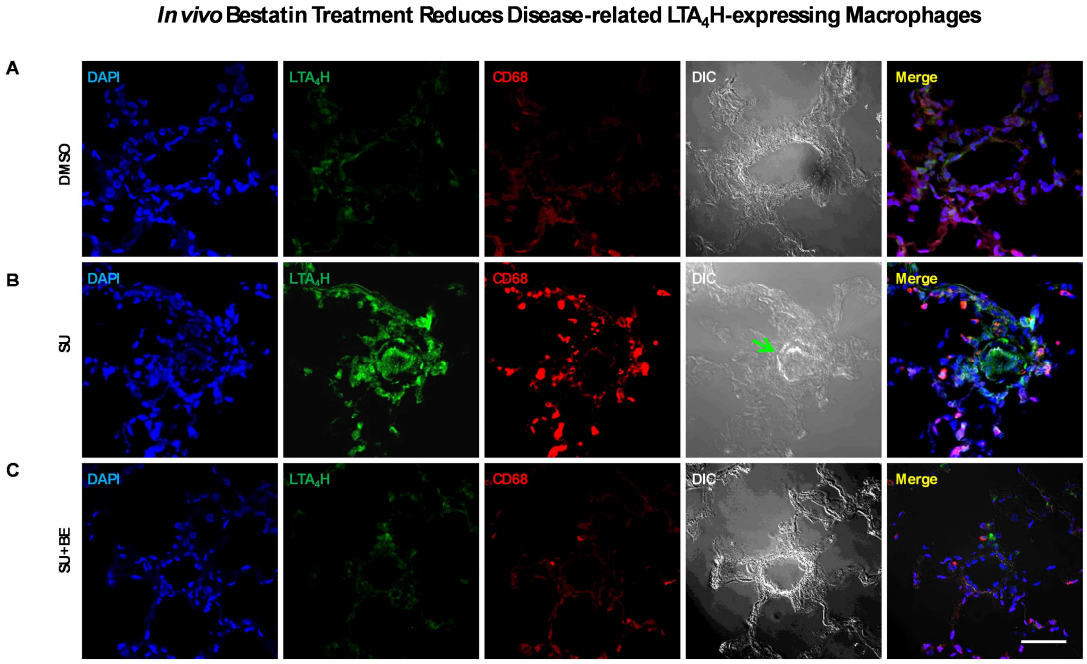

Fig. S20. Reduction of disease-related LTA_4H expression in macrophages in bestatin-treated rats. (**A** to **C**) Representative immunofluorescence images from lung sections stained with LTA_4H (green) and CD68 (red), with or without bestatin treatment demonstrate reduced LTA_4H expression in macrophages. DAPI (blue), nuclei. Differential interference contrast (DIC) highlights small arteriole structural features. Green arrow, occluded vessel; N=6 per group; scale bar, 50μm.

Fig. S21. *In Vivo* Bestatin Treatment Reduces Lung Inflammation

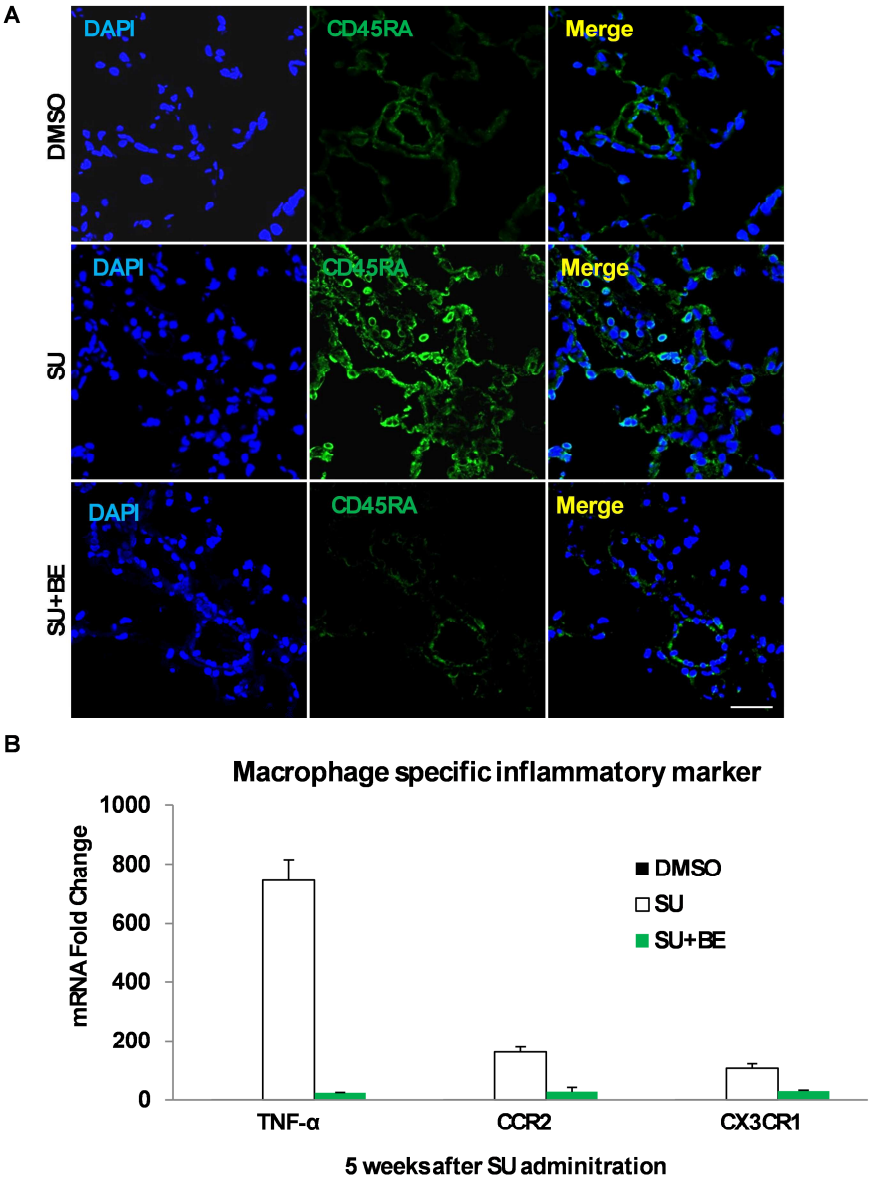

Fig. S21. Inflammation attenuation in bestatin-treated animals. (**A**) Lung sections from DMSO, SU and bestatin-treated animals at wk 5 were stained with CD45RA (green) to assess B cell infiltration. Representative confocal images are shown. DAPI (blue), nuclei. N=6 per group; scale bar, 50μm. (**B**) The macrophage-associated cytokine TNF-α, and chemokines, CXCR1 and CCR2 in PH was evaluated by RT-PCR of lung tissues. N=3 experiments per group. Data are expressed as means ± s.e.m..

Fig. S22.

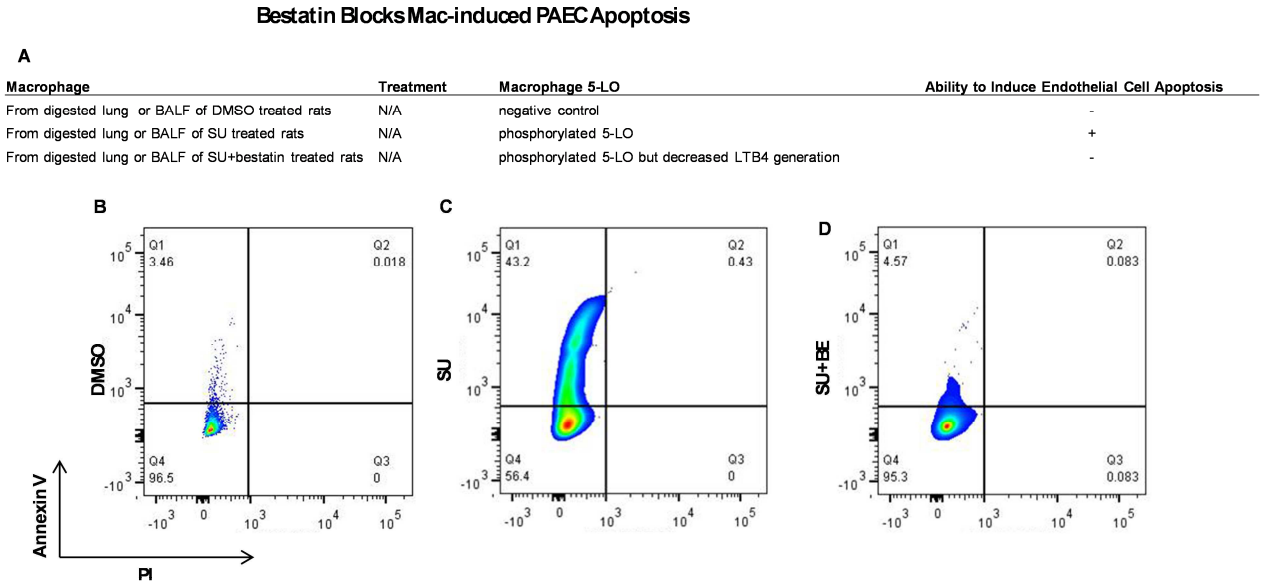

Fig. S22. Prevention of PH lung macrophage–induced PAEC apoptosis with bestatin. (**A**) To investigate the effect of bestatin on macrophage-induced endothelial cell apoptosis, lung macrophages, from DMSO, SU and bestatin-treated rats were isolated, and cocultured with PAECs for 24hr. Macrophages from healthy rats transfected with S271E mutant were treated with 30μM of bestatin for 4hr, then were cocultured with PAECs for 24hr before testing. Results were summarized. (**B** to **D**) Flow cytometry was used to assess PAEC apoptosis. N=3 experiments per group.

Fig. S23.

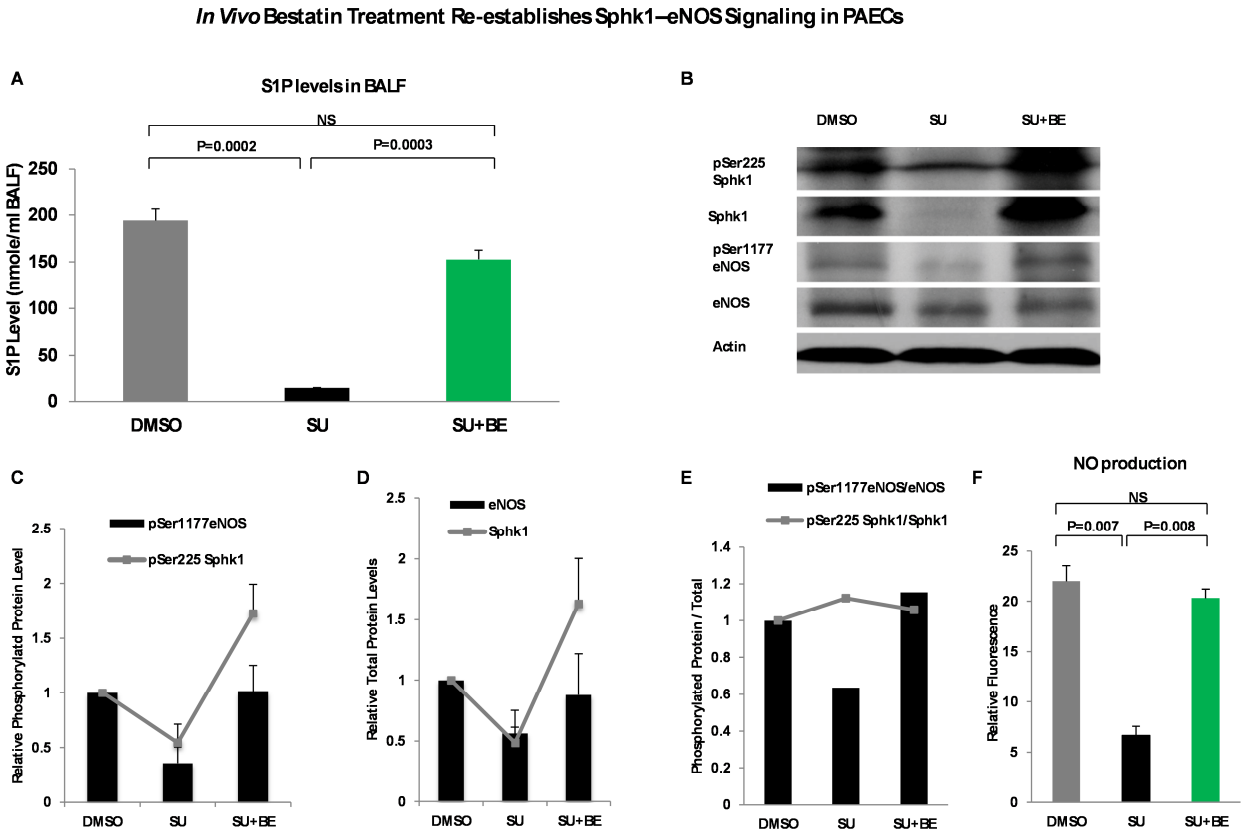

Fig. S23. Reestablishing lung Sphk1-eNOS signaling with bestatin treatment in established PH. (**A**) LC-MS/MS results demonstrate normalized S1P levels in the BALF after bestatin treatment. (**B** to **D**) Western blot data from endothelial cells cocultured with macrophages that were obtained from the lungs of control, SU and bestatin-rescued PH lungs. (**E**) Ratio of phospho protein and total protein was calculated. (**F**) Normalized NO production was measured by DAF-2DA relative fluorescence of coculture media. N=4 experiments per group. Kruskall-Wallis test followed by Dunn's multiple comparisons test for post hoc analyses were used. Data are expressed as means ± s.e.m.. NS, not significant.

Fig. S24.

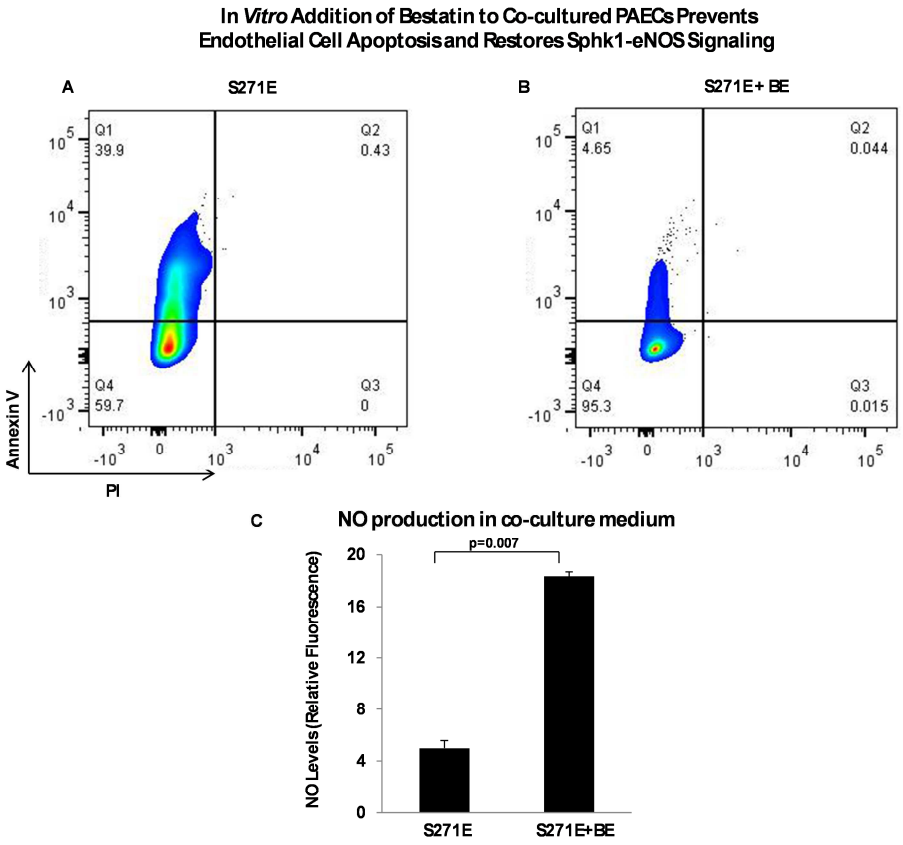

Fig. S24. Prevention of mutant-mimic macrophage-induced PAEC apoptosis and maintenance of Sphk1-eNOS signaling with exogenous bestatin. Macrophages from healthy rats transfected with S271E mutant were treated with 30µM bestatin for 4hr, were then cocultured with PAECs for 24hr before testing. (**A** and **B**). Bestatin prevented endothelial cell apoptosis induced by LTB_4 generated by 5-LO phosphorylation in macrophages. (**C**) Normalized NO was measured by DAF-2DA relative fluorescence. N=3 experiments per group. Kruskall-Wallis test followed by Dunn's multiple comparisons test for post hoc analyses were used. Data are expressed as means ± s.e.m..

Fig. S25.

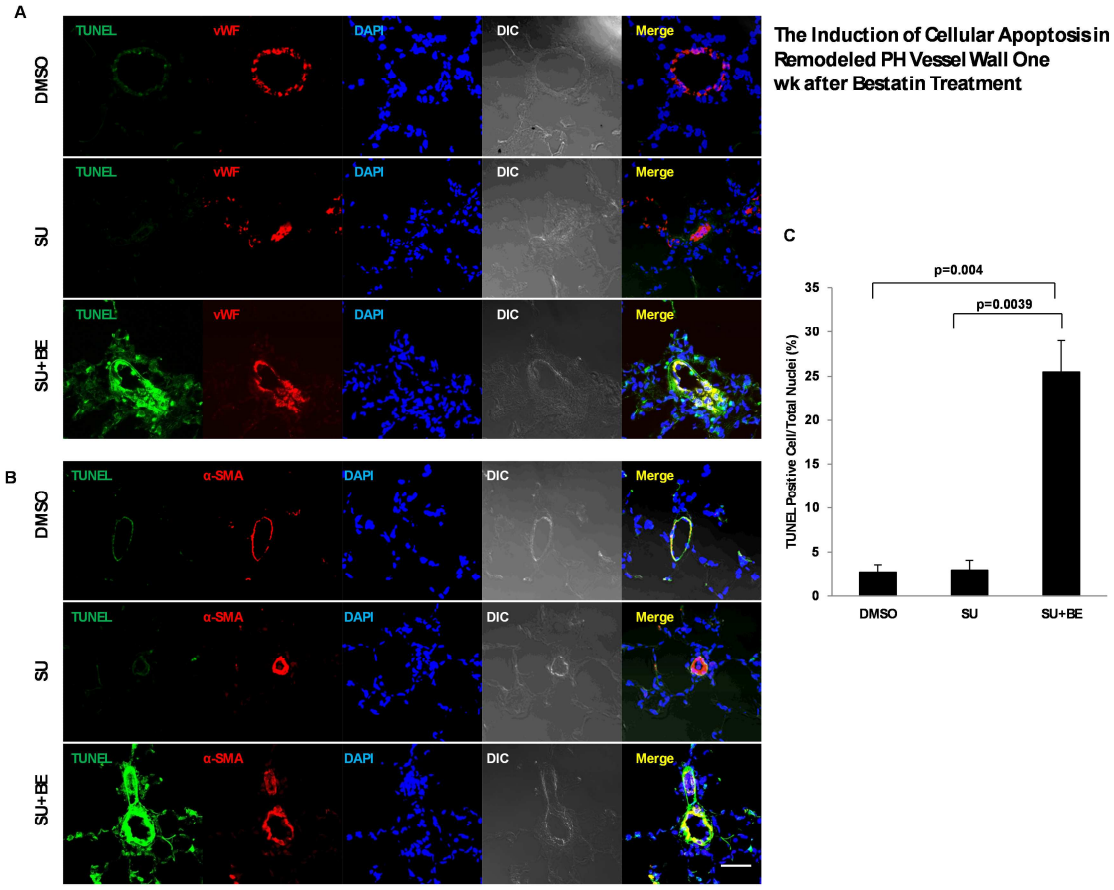

Fig. S25. The induction of cellular apoptosis in remodeled PH vessel wall 1 week after bestatin treatment. (A to **C)**Representative fluorescence images of apoptotic cell identified by terminal deoxynucleotidyl transferase-mediated deoxyuridine triphosphate nick end-labeling (TUNEL, green) co-stained with (**A**) vWF (red) or (**B**) *a*-SMA (red). (**C**) Ratio of TUNEL-positive cells to total nuclei in each group. DAPI (blue), nuclei; N=6 per group; scale bar, 50 μm. Kruskall-Wallis test followed by Dunn's multiple comparisons test for post hoc analyses were used. Data are expressed as means ± s.e.m..

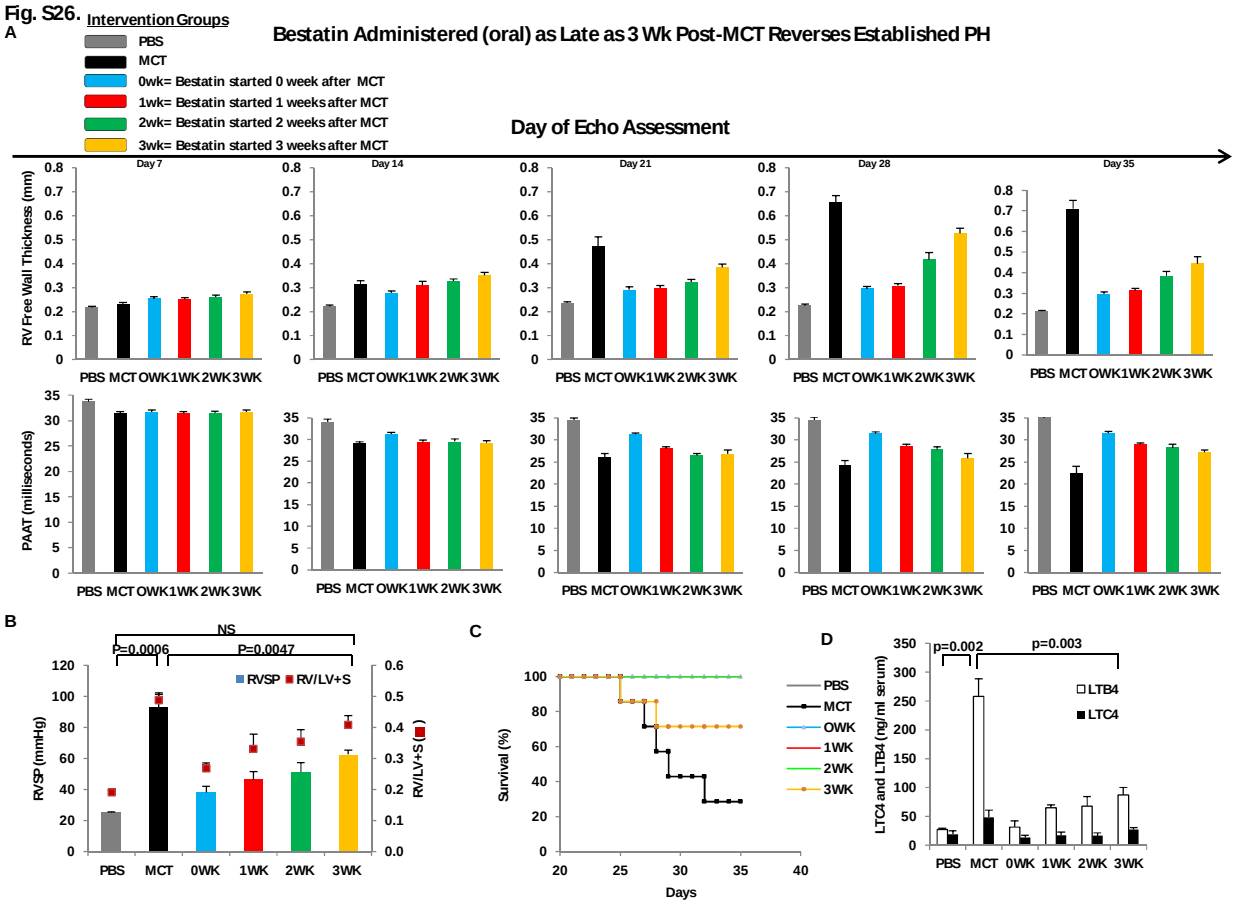

Fig. S26. The reversal of PH in the MCT model using bestatin therapy. Rats were given 1mg/kg bestatin oral daily starting 0 wk, 1 wk, 2 wk or 3 wk after MCT administration. Animals were monitored by echocardiography (ECHO) weekly, and sacrificed for hemodynamics measurement at wk 5. (**A**) Sequential ECHO of saline, MCT, bestatin (0 wk after MCT), bestatin (1wk after MCT), bestatin (2wk after MCT), and bestatin (3wk after MCT) treatment groups illustrating respective RV free wall thicknesses and PAAT. (**B**) RVSP and RVH were measured in saline, MCT, and 4 different bestatin protocols at wk 5 post-MCT administration. (**C**) Survival of rats after bestatin treatment was compared with MCT and saline. Bestatin-treated groups overlap with the PBS (negative control), 0WK, 1WK, and 2WK groups. (**D**) Serum LTB_4 and LTC_4 concentration was measured in each group. N=7 per group. Two-way ANOVA with Bonferroni multiple comparisons test for post hoc analyses were used. Data are expressed as means ± s.e.m.. NS, not significant.

Fig. S27.

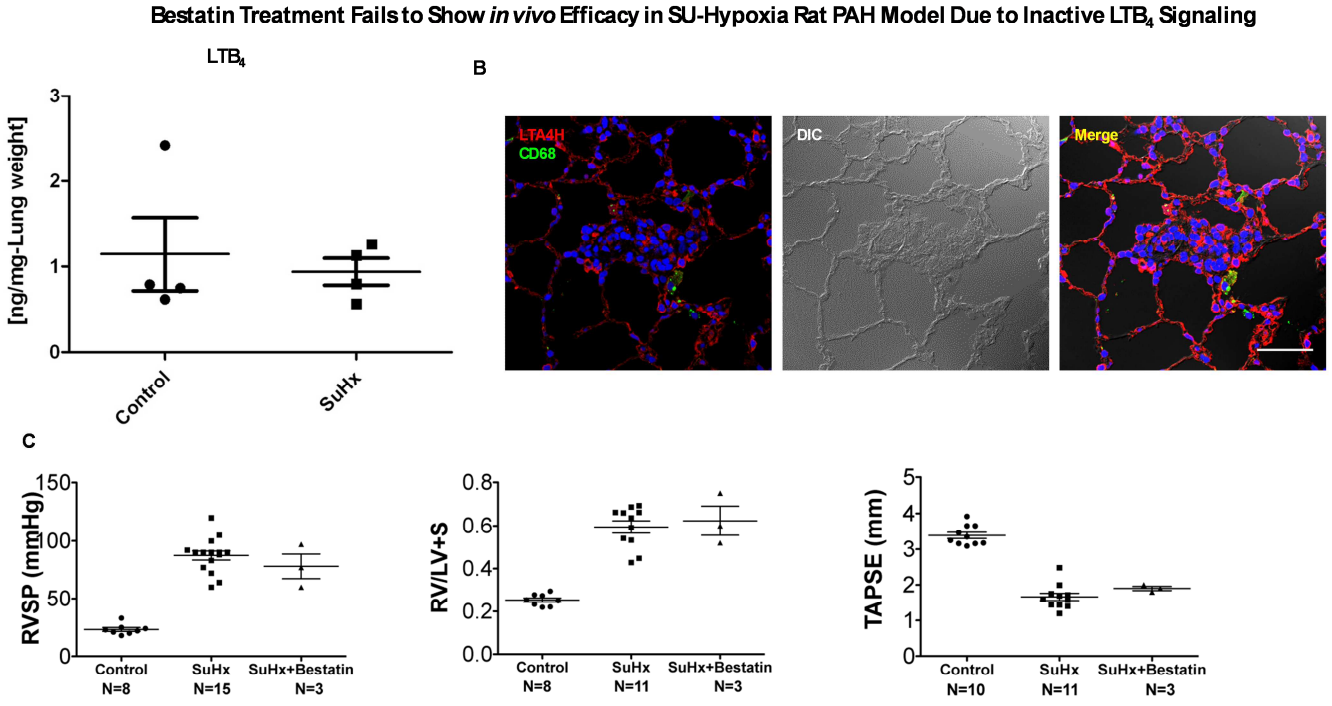

Fig. S27. The failure of bestatin in the low-LTB_4 SU/hypoxia PH model. (**A**) LC-MS/MS results demonstrate normalized LTB_4 levels in the BALF in control and SU5416-Hypoxia (SuHx) groups. (**B**) Representative confocal images of SuHx rat lung tissues stained with CD68 (green) and LTA_4H (red) reveal few macrophage infiltrates and normal LTA_4H expression. DAPI (blue) identifies nuclei. Differential interference contrast (DIC) highlights small arteriole structural features. N=6 per group; scale bar, 50μm. (**C**) Hemodynamic measurements using RVSP and RV/LV+S; RV functional index TAPSE (tricuspid annular plane systolic excursion) demonstrate no in vivo efficacy of bestatin. Numbers of animals in different groups are listed in each panel. Data are presented as means ± s.e.m..

Table S1.

Hemodynamic and Echocardiography Data for Athymic Rats at Different Time Points after SU Administration

Number of weeks following SU injection	RVSP(mmHg)	RV/LV+S	PAAT(milliseconds)	RV free wall thickness(mm)
0 wk	25±5	0.23±0.05	33±5	0.22±0.06
1 wk	36±10	0.32±0.15	28±6	0.35±0.09
2 wk	47±15	0.53±0.13	22±10	0.57±0.10
3 wk	65±13	0.64±0.08	15±7	0.71±0.19
4 wk	80±14	0.72±0.12	10±8	1.07±0.17

Table S2.

Dosing Regimen for Different Eicosanoid Inhibitors

Drug	Dosage (mg/kg)	Route of Administration
Bestatin	0.25,0.5,0.75 or 1	P.O. Daily
JNJ	30	P.O. Twice a Day
ATK	5	P.O. Daily
MK886	5	P.O. Daily
Aspirin	100	P.O. Daily
Zileuton	30	P.O. Twice a Day
Montelukast	10	P.O. Daily
DCU	30	P.O. Daily
LY293111	0.5	P.O. Daily